Revista Mexicana de Física **38**, *No. 3 (1992) 343–397*

Enhanced backscattering from one- and two-dimensional random surfaces

A.A. MARADUDIN, JUN Q. LU, P. TRAN, R.F. WALLIS
Department of Physics and Institute for Surface and Interface Science
University of California, Irvine, CA 92717, U.S.A.

V. CELLI
Department of Physics, University of Virginia
Charlottesville, VA 22901, U.S.A.

ZU-HAN GU
Surface Optics Corporation
P.O. Box 261602, San Diego, CA, U.S.A.

A.R. MCGURN
Department of Physics, Western Michigan University
Kalamazoo, MI 49008, U.S.A.

E.R. MÉNDEZ
División de Física Aplicada, CICESE
Apartado postal 2732, Ensenada, Baja California, Mexico

T. MICHEL
School of Physics, Georgia Institute of Technology
Atlanta, GA 30332, U.S.A.

M. NIETO-VESPERINAS
Instituto de Optica, C.S.I.C.
Serrano 121, Madrid 28006, Spain

J.C. DAINTY AND A.J. SANT
Applied Optics Section, Blackett Laboratory
Imperial College of Science, Technology and Medicine
London, SW72AZ, United Kingdom

Recibido el 19 de septiembre de 1991; aceptado el 16 de enero de 1992

ABSTRACT. The enhanced backscattering of light from a random surface is manifested by a well-defined peak in the retroreflection direction in the angular distribution of the intensity of the incoherent component of the light scattered from such a surface. In this article we present a survey of recent theoretical and experimental results concerning the enhanced backscattering of light from one- and two-dimensional random surfaces on metallic, dielectric, and perfectly conducting

substrates, which bear on the conditions under which this phenomenon occurs and on the way it depends on the nature of the random roughness. We consider not only the case in which the random surface bounds a semi-infinite scattering medium but also the case in which it bounds a film, either free-standing or on a reflecting substrate. It is shown that several effects occur in the latter structures that are absent from their semi-infinite counterparts.

RESUMEN. La retrodispersión reforzada de luz por una superficie aleatoria se manifiesta en la distribución angular de intensidades de la componente incoherente de la luz dispersada por la superficie, en forma de un pico bien definido en la dirección de retrorreflexión. En este trabajo presentamos una revisión de resultados recientes tanto teóricos como experimentales referentes a la retrodispersión reforzada de luz por superficies aleatorias uni- y bidimensionales sobre sustratos metálicos, dieléctricos y perfectamente conductores, prestando atención a las condiciones bajo las cuales ocurre el fenómeno y a la forma en que depende de la naturaleza de la irregularidad de la superficie. Consideramos tanto el caso en que la superficie delimita un medio dispersivo semiinfinito, como el caso en que delimita una película, ya sea libre o sobre un sustrato reflector. Se muestra que en estas últimas estructuras ocurren varios efectos que estaban ausentes de su contraparte semiinfinita.

PACS: 73.90.+f

1. INTRODUCTION

One of the interesting new effects associated with the scattering of light from a random surface is that of enhanced backscattering. This effect is the presence of a well-defined peak in the retroreflection direction in the angular dependence of the contribution to the mean differential coefficient from the incoherent component of the scattered light. Since its theoretical prediction [1] it has been studied intensively both theoretically [2-24] and experimentally [25-30]. On the basis of these studies it is now believed that the enhanced backscattering of light from a moderately rough, reflecting random surface is due primarily to the coherent interference of each multiply-reflected optical path with its time-reversed partner, with the dominant contribution coming from the doubly-reflected paths. If the scattering surface supports surface electromagnetic waves, enhanced backscattering is observed from even weakly corrugated surfaces [1-3]. In this case it is due primarily to the coherent interference of each multiply-scattered surface electromagnetic wave path with its time-reversed partner. Again, the dominant contribution to this effect appears to come from the doubly-scattered wave paths.

Enhanced backscattering is an example of a broader class of multiple-scattering phenomena that go under the name of *weak localization*. This name originated in earlier theoretical studies of the conduction of electrons in disordered materials, in which it was found that this transport process is affected by coherent effects in the electronic wave function, not taken into account in the standard Boltzmann transport equation for this process, when the mean free path between consecutive collisions of an electron with the impurities becomes shorter than their wavelength. These coherent effects produce an enhanced probability for an electron to return to its origin, *i.e.*, an enhanced backscattering of the electron [31,32]. The enhanced probability of return to the origin reduces the diffusion constant of the electron, and consequently the electrical conductivity of the disordered material. The enhanced backscattering of the electron, and the decrease in

its diffusion constant that it causes, are called weak localization [33]. When the concentration of impurities becomes very dense, and the scattering from each impurity is very strong, electrical conduction will vanish at absolute zero temperature. The vanishing of electrical conduction under these conditions is called *strong localization* or *Anderson localization* [34].

Although it had its origins in studies of the propagation of an electron in a random medium, weak localization is now recognized to be a general property of all waves propagating in such a medium, including classical waves such as electromagnetic waves, elastic waves, and acoustic waves [35]. The enhanced backscattering of light in volume scattering has been observed when the random system is an aqueous suspension of polystyrene microspheres [36-38]. It was first interpreted as due to the coherent interference between time-reversed light paths by Tsang and Ishimaru [39], and its connection with weak localization was first pointed out by van Albada and Lagendijk [37]. Consequently, it is natural to associate the enhanced backscattering of light from a moderately rough, reflecting surface with the weak localization of light, and the enhanced backscattering of light from weakly corrugated surfaces that support surface electromagnetic waves with the weak localization of those surface electromagnetic waves. There is, however, an important difference between the enhanced backscattering of light from volume systems, such as polystyrene microspheres in water, and the enhanced backscattering of light in reflection from a random surface: whereas the former can require several hundred, or even a few thousands of, collisions of the light with the randomly distributed scattering centers to form a well-defined enhanced backscattering peak [40], the latter requires only very few reflections of the light from the random surface, to accomplish the same result. Two reflections are necessary, and nearly sufficient.

In this article we review some recent results and present some new results concerning the enhanced backscattering of light from weakly and strongly corrugated, one- and two-dimensional, random surfaces on metallic, dielectric, and perfectly conducting substrates. These explore both the conditions under which this phenomenon occurs and the way in which it depends on the nature of the random surface.

The surfaces we study are all planar in the absence of the random roughness, and we assume that the plane perturbed by the roughness is the plane $x_3 = 0$. We first consider the scattering of light from one-dimensional random surfaces, *i.e.*, from surfaces defined by the equation $x_3 = \zeta(x_1)$, where the surface profile function $\zeta(x_1)$ is a function of only one of the two coordinates in the plane $x_3 = 0$. We begin by examining the manner in which enhanced backscattering depends on the nature of the surface profile function $\zeta(x_1)$. We first consider one-dimensional, random surfaces characterized by a single transverse length scale and defined by four different surface height correlation functions *viz.* a Lorentzian, a Gaussian, a $(\sin c)^2$, and a $\sin c$ function of (x_1/a) where a defines the transverse correlation length scale of the surface roughness. The surface structure factors (power spectra) corresponding to these height correlation functions decay to zero progressively more rapidly in wave number space. Enhanced backscattering and subsidiary maxima are observed in the angular dependence of the intensity of the light scattered from each of these surfaces, and features of the mean differential reflection coefficient are correlated with the mean distance between consecutive peaks and valleys on each of these surfaces, $\langle d \rangle$, and the standard deviation of this quantity. It is also shown that the angular width of

the enhanced backscattering peak is inversely proportional to the mean distance between consecutive peaks and valleys on the surface in the case of the Gaussian height correlation function. The gradual disappearance of the subsidiary maxima as the ratio $\lambda/\langle d\rangle$ increases, where λ is the wavelength of the incident light, is demonstrated and discussed.

In contrast with the preceding investigations, which are based on surface profile functions characterized by a single transverse length scale, we have also investigated by numerical simulations, the scattering of both p- and s-polarized light from a one-dimensional, randomly rough, metallic surface whose surface structure factor is a truncated Lorentzian. The resulting surface can be termed a band limited fractal. The angular width of the enhanced backscattering peak is found to increase with an increase in the cutoff wave number in the surface structure factor, at the same time that the mean distance $\langle d\rangle$ between consecutive maxima on the surface decreases. In fact, the angular width is found to depend inversely on $\langle d\rangle$, and becomes large enough for the peak to be indistinguishable from the background when $\langle d\rangle$ is sufficiently small.

The results of these two investigations are important for demonstrating that enhanced backscattering is due to interference (and hence cannot be a single-scattering effect) and thus indeed is a weak localization effect.

A commonly made assumption about the surface profile $\zeta(x_1)$ is that it is a Gaussianly distributed random variable. We demonstrate that this is not a necessary condition for the occurrence of enhanced backscattering by showing theoretically that light scattered from a random surface defined by a surface profile function that is not a Gaussianly distributed random variable also displays enhanced backscattering.

We next explore the consequences of relaxing the assumption that the surface profile function is a stationary stochastic process. We do this by studying the scattering of p-polarized light from random metallic gratings characterized by surface profile functions $\zeta(x_1)$ that are even and odd functions of x_1. They are therefore not stationary stochastic processes. For both types of profiles enhanced backscattering is found. In the case of scattering from surfaces characterized by even profile functions an enhanced scattering in the specular direction is also observed in the angular distribution of the intensity of the incoherent component of the scattered light. The latter occurs even in the Kirchhoff approximation, and hence is not primarily due to multiple scattering.

Since the enhanced backscattering of light from weakly corrugated random surfaces that support surface polaritons is believed to be due primarily to the coherent interference of each surface polariton double-scattering sequence that contributes to backscattering with its time-reserved partner, any mechanism that breaks the time reversal symmetry of the scattering system should degrade the enhanced backscattering from it. A static magnetic field applied parallel to the grooves of a random grating on the surface on an n-type semiconductor does so, with the result that the dispersion curve of surface polaritons supported by such surfaces becomes nonreciprocal. We present the results of numerical simulation studies of enhanced backscattering from metal and semiconducting surfaces which show that the position of the backscattering peak moves toward larger scattering angles with increasing magnetic field strength, and the peak itself also broadens and eventually disappears.

In addition, if a way can be found to eliminate surface polaritons with frequencies within a certain range from a random surface, then light whose frequency falls within

this range should not produce an enhanced backscattering peak when it is scattered from that surface. A periodic grating ruled on a metal surface opens up a gap in the dispersion curve of the surface polaritons supported by that surface. When the periodically corrugated surface is further roughened randomly, we show by computer simulations that the enhanced backscattering of light whose frequency lies within that gap is strongly suppressed by the absence of surface polaritons in this frequency range.

In earlier work [11] it was shown that enhanced backscattering is not observed in the scattering of p-polarized light from a random grating of large rms slope on the surface of a semi-infinite, nearly transparent, dielectric medium. We present theoretical and experimental results which demonstrate that if the dielectric material is deposited as a film on the planar surface of a highly reflecting substrate, *e.g.*, a perfect conductor or a metal, a well-defined enhanced backscattering peak is observed in this polarization. In fact, it is not necessary to deposit the dielectric film on a reflecting substrate in order to induce enhanced backscattering from a randomly rough dielectric surface. Enhanced backscattering is observed in the scattering of p-polarized light from a free-standing dielectric film whose illuminated surface is randomly rough and whose back surface is planar. In both cases, the enhanced backscattering is due to the coherent interference of a light path that passes through the rough surface twice due to its reflection from the back surface of the film, and its time-reserved partner.

Finally, we present theoretical results for the enhanced backscattering that occurs in the in-plane cross-polarized scattering of p- and s-polarized light incident normally on weakly corrugated, two dimensional, random metallic and strongly reflecting surfaces. These are surfaces whose surface profile function $\zeta(x_1, x_2)$ is a function of both of the coordinates in the plane band $x_3 = 0$. The calculations are carried out by constructing a randomly rough surface in the square region $-\frac{1}{2}L, < x_1, x_2 < \frac{1}{2}L$, replicating it periodically, and using the theory of light scattering from bigratings [41-43] based on the method of reduced Rayleigh equations [44] to solve for the scattered fields. It is shown that the planar interface between vacuum and the metal or strongly reflecting dielectric supports surface electromagnetic waves, whose weak localization by the random roughness gives rise to the enhanced backscattering.

2. ONE-DIMENSIONAL RANDOM SURFACES ON SEMI-INFINITE MEDIA

In this section we describe two investigations of enhanced backscattering from one-dimensional random surfaces on semi-infinite media that explore in turn the mechanisms underlying this effect for moderately rough, reflecting surfaces and for weakly rough surfaces that support surface electromagnetic waves.

Until recently the theoretical study of the scattering of light from one-dimensional random surfaces might have appeared to be a largely academic endeavor. On the one hand the early interest in the scattering of electromagnetic waves from random surfaces was prompted to a large extent by such practical problems as the propagation of radar over an ocean surface, or the propagation of radio waves over the earth's terrain, in which cases the rough surfaces of interest were manifestly two-dimensional. On the other hand, the technology for producing one-dimensional random surfaces with root-mean-square

heights and transverse correlation lengths of the order of the wavelength of the incident light did not exist. Consequently, the scattering of light from one-dimensional random surfaces was studied theoretically largely because such surfaces are easier to work with than the more realistic two-dimensional surfaces, since scattering of incident light of p- or s-polarization from such surfaces occurs without change of polarization when the plane of incidence, and hence the plane of scattering, is normal to the generators of the surface. Nevertheless, the results of such studies could provide insights into the more difficult problem of the scattering of light from two-dimensional random surfaces.

With the development of methods for producing one-dimensional random surfaces with specified surface height correlation functions and specified surface height probability distribution functions [28,45,46], the situation has changed. It is now possible to study experimentally the scattering of light from one-dimensional random surfaces on metal and nearly transparent substrates [28,29,30,47,48], and the results of such studies provide a testing ground for theories of such scattering.

Thus, in this section the physical system we consider consists of vacuum in the region $x_3 > \zeta(x_1)$ and a dielectric medium in the region $x_3 < \zeta(x_1)$. The surface profile function $\zeta(x_1)$ is assumed to be a single-valued, continuous, differentiable function of x_1, and to constitute a *stationary, Gaussian*, stochastic process. The words "stationary" and "Gaussian" have been italicized here, because both of these assumptions will be relaxed in some of the work described in what follows. This process is defined by the properties $\langle \zeta(x_1) \rangle = 0$ and $\langle \zeta(x_1)\zeta(x_1') \rangle = \delta^2 W(|x_1 - x_1'|)$, where the angle brackets denote an average over the ensemble of realizations of the surface profile, while $\delta = \langle \zeta(x_1)) \rangle^{1/2}$ is the root-mean-square departure of the surface from flatness. (A more general form for $\zeta(x_1)$ will be assumed in Sect. 2.2.2 below.) The surface height correlation function $W(|x_1|)$ will be specified below for each of the surfaces studied. The surface structure factor, or the power spectrum of the surface roughness, $g(|Q|)$ is defined as the Fourier transform of $W(|x_1|)$,

$$g(|Q|) = \int_{-\infty}^{\infty} dx_1 e^{-iQx_1} W(|x_1|). \tag{2.1}$$

We will study the scattering of p- and s-polarized beams of light of finite width, incident from the vacuum side onto a random surface of this type of length L. The plane of incidence is the x_1x_3-plane. By choosing the width of the incident beam suitably, we make the amplitude of the beam at the ends of the rough segment of the scattering surfaces sensibly zero. Consequently it is not necessary to replicate the rough portion of the surface periodically [6,49].

In the case of the scattering of a p-polarized beam of light we will work with the single, nonzero component of the magnetic vector of the electromagnetic field, $H_2(x_1, x - 3|\omega)$. A time dependence of $exp(-i\omega t)$ is assumed. The incident beam then has the form

$$H_2^{>}(x_1, x_3|\omega)_{inc} = \exp\left\{i\frac{\omega}{c}(x_1 \sin\theta_0 - x_3 \cos\theta_0)[1 + w(x_1, x_3)]\right\}$$
$$\times \exp[-(x_1 \cos\theta_0 + x_3 \sin\theta_0)^2/w^2], \tag{2.2}$$

where $w(x_1, x_3) = [c^2/(\omega^2 w^2)]\{[2(x_1 \cos\theta_0 + x_3 \sin\theta_0)^2/w^2] - 1\}$. Here θ_0 is the angle of incidence measured from the normal to the mean surface $x_3 = 0$, and w is the half-width of the beam. The half-width of the intercept of the beam with the plane $x_3 = 0$ is $g = w/\cos\theta$. We will use values of L/g of the order of 4–5 in the calculations described in this paper.

By the use of Green's second integral theorem [50] it can be shown that the contribution to the mean differential reflection coefficient from the incoherent component of the scattered light is given exactly by [12]

$$\left\langle \frac{\partial R_p}{\partial \theta_s} \right\rangle_{\text{incoh}} = \frac{1}{2(2\pi)^{3/2}} \frac{c}{\omega w} \frac{\langle |r_p(\theta_s)|^2 \rangle - |\langle r_p(\theta_s) \rangle|^2}{[1 - c^2(1 + 2\tan^2\theta_0)/(2\omega^2 w^2)]}, \quad |\theta_s| \leq \frac{\pi}{2}, \tag{2.3}$$

where θ_s is the angle of scattering, measured from the normal to the surface $x_3 = 0$. The first term on the right hand side of Eq. (2.3) by itself gives the total mean differential reflection coefficient. The second term is the contribution to the mean differential reflection coefficient from the coherent component of the scattered light. Since in the study of enhanced backscattering it is the contribution to the mean differential reflection coefficient from the incoherent component of the scattered light that is of interest, we work the difference displayed in Eq. (2.3).

The scattering amplitude $r_p(\theta_s)$ in Eq. (2.3) is

$$r_p(\theta_s) = \int_{-\infty}^{\infty} dx_1 e^{i\frac{\omega}{c}[x_1 \sin\theta_s + \zeta(x_1)\cos\theta_s]} \times \left\{ i\frac{\omega}{c}[\zeta'(x_1)\sin\theta_s - \cos\theta_s] H(x_1|\omega) - L(x_1|\omega) \right\} \tag{2.4}$$

where the source functions $H(x_1|\omega)$ and $L(x_1|\omega)$ are the boundary values of the total magnetic field in the vacuum and of its normal derivative,

$$H(x_1|\omega) = H_x^{>}(x_1, x_2|\omega)|_{x_3 = \zeta(x_1)}, \tag{2.5a}$$

$$L(x_1|\omega) = \left(-\zeta'(x_1)\frac{\partial}{\partial x_1} + \frac{\partial}{\partial x_3} \right) H_2^{>}(x_1, x_3|\omega)\Big|_{x_3 = \zeta(x_1)} \tag{2.5b}$$

These functions satisfy the pair of coupled integral equations

$$H(x_1|\omega) = H(x_1|\omega)_{\text{inc}} + \int_{-\infty}^{\infty} dx_1' [H_0(x_1|x_1')H(x_1'|\omega) + L_0(x_1|x_1')L(x_1'|\omega)], \tag{2.6a}$$

$$0 = \int_{-\infty}^{\infty} dx_1' [H_\epsilon(x_1|x_1')H(x_1'|\omega) - \epsilon(\omega)L_\epsilon(x_1|x_1')L(x_1'|\omega)], \tag{2.6b}$$

where $H(x_1|\omega)_{\text{inc}} = H_2^{>}(x_1, \zeta(x_1)|\omega)_{\text{inc}}$, $\epsilon(\omega)$ is the complex dielectric constant of the scattering medium, and

$$H_\epsilon(x_1|x_1') = \lim_{\epsilon\to 0+}\left(\frac{-i}{4}\right) n_c^2 \frac{\omega^2}{c^2} \frac{H_1^{(1)}\left(n_c\frac{\omega}{c}[(x_1 - x_1')^2 + (\zeta(x_1)) - \zeta(x_1') + \epsilon)^2]^{1/2}\right)}{n_c\frac{\omega}{c}[(x_1 - x_1')^2 + (\zeta(x_1) - \zeta(x_1') + \epsilon)^2]^{1/2}}$$

$$\times [(x_1 - x_1')\zeta(x_1') - (\zeta(x_1) - \zeta(x_1') + \epsilon)], \tag{2.7a}$$

$$L_\epsilon(x_1|x_1') = \lim_{\epsilon\to 0+}\left(\frac{i}{4}\right) H_0^{(1)}\left(n_c\frac{\omega}{c}[(x_1 - x_1')^2 + (\zeta(x_1) - \zeta(x_1') + \epsilon)^2]^{1/2}\right). \tag{2.7b}$$

In these expressions $n_c = (\epsilon(\omega))^{1/2}$ is the complex index of refraction of the scattering medium, and we require that $\operatorname{Re} n_c > 0$, $\operatorname{Im} n_c > 0$; $H_0^{(0)}(z)$ and $H_1^{(1)}(z)$ are Hankel functions. The kernels $H_0(x_1|x_1')$ and $L_0(x_1|x_1')$ in Eqs. (2.6) are obtained by setting $n_c = 1$ in Eqs. (2.7*a*) and (2.7*b*), respectively.

In the case of the scattering of an s-polarized beam of light we work with the single nonzero component of the electromagnetic field in the system, $E_2(x_1, x_3|\omega)$. The incident field is now given by

$$E_2^{>}(x_1, x_3|\omega)_{\text{inc}} = \exp\left\{i\frac{\omega}{c}(x_1 \sin\theta_0 - x_3\cos\theta_0)[1 + w(x_1, x_3)]\right\}$$

$$\times \exp[-(x_1\cos\theta_0 + x_3\sin\theta_0)^2/w^2] \tag{2.8}$$

The contribution to the mean differential reflection coefficient from the incoherent component of the scattered light is given by [12]

$$\left\langle\frac{\partial R_s}{\partial\theta_s}\right\rangle_{\text{incoh}} = \frac{c}{2(2\pi)^{3/2}}\frac{c}{\omega w}\frac{\langle|r_s(\theta_s)|^2\rangle - |\langle r_s(\theta_s)\rangle|^2}{[1 - c^2(1 + 2\tan^2\theta_0)/(2\omega^2 w^2)]}; \quad |\theta_s| \le \frac{\pi}{2}, \tag{2.9}$$

where the scattering amplitude $r_s(\theta_s)$ is

$$r_s(\theta_s) = \int_{-\infty}^{\infty} dx_1 \exp\left(i\frac{\omega}{c}[x_1\sin\theta_s + \zeta(x_1)\cos\theta_s]\right)$$

$$\times\left\{i\frac{\omega}{c}[\zeta'(x_1)\sin\theta_s - \cos\theta_s]E(x_1|\omega) - F(x_1|\omega)\right\}. \tag{2.10}$$

The source functions $E(x_1|\omega)$ and $F(x_1|\omega)$ entering this expression are the boundary values of the total electric field in the vacuum and of its normal derivative,

$$E(x_1|\omega) = E_2^{>}(x_1, x_3|\omega)|_{x_3=\zeta(x_1)}, \tag{2.11a}$$

$$F(x_1|\omega) = \left(-\zeta'(x_1)\frac{\partial}{\partial x_1} + \frac{\partial}{\partial x_3}\right) E_2^{>}(x_1, x_3|\omega)\Big|_{x_3=\zeta(x_1)} \tag{2.11b}$$

They satisfy the following pair of coupled integral equations:

$$E(x_1|\omega) = E(x_1|\omega)_{\text{inc}} + \int_{-\infty}^{\infty} dx_1'[H_0(x_1|x_1')E(x_1'|\omega) - L_0(x_1|x_1')F(x_1|\omega)], \quad (2.12a)$$

$$0 = \int_{-\infty}^{\infty} [H_\epsilon(x_1|x_1')E(x_1'|\omega) - L_\epsilon(x_1|x_1')F(x_1'|\omega)], \quad (2.12b)$$

where $E(x_1|\omega)_{\text{inc}} = E_2^>(x_1, \zeta(x_1)|\omega)_{\text{inc}}$.

In solving the pairs of coupled integral equations (2.6) and (2.12) the infinite range of integration in each equation was replaced by the finite range $(-L/2, L/2)$, and the latter was divided into N equal intervals. The values of $\zeta(x_1)$ and its derivatives were calculated at the midpoints of these intervals by the method described in Appendix A of Ref. [12]. The integral equations were then solved by the method of moments [51].

The scattering amplitude $r(\theta_s)$, either $r_p(\theta_s)$ or $r_s(\theta_s)$, was then calculated for each of N_p different surface profiles. The results were summed over the N_p realizations of $\zeta(x_1)$ and the sum was divided by N_p to yield the function $\langle r(\theta_s)\rangle$. Similarly, the squared modulus of $r(\theta_s)$ was calculated for each of the N_p realizations of $\zeta(x-1)$, the results were summed and the total divided by N_p to yield the function $\langle |r(\theta_s)|^2\rangle$. From these two functions the contribution to the mean differential reflection coefficient from the incoherent component of the scattered light was calculated from Eqs. (2.3) and (2.9).

In this section we apply this approach to several investigations of the enhanced backscattering of light from one-dimensional random surfaces that explore in turn some of the conditions under which this phenomenon occurs for moderately rough, reflecting surfaces, and for weakly rough surfaces that support surface electromagnetic waves.

2.1 The dependence of enhanced backscattering on the nature of the surface height correlation function

It is generally accepted today that the enhanced backscattering of light from a moderately rough, reflecting, random surface arises in the following way [11,25,26]. The incident light striking the surface undergoes $n-1$ $(n > 1)$ additional reflections from it, at the last of which it is scattered back into the vacuum away from the surface. All such n-order scattering sequences are uncorrelated due to the random nature of the surface profile. However, any given sequence and its time-reversed partner, in which the light is reflected from the same points on the surface but in the reverse order, interfere constructively if the wave vectors of the incident and final waves are oppositely directed. These two waves have the same amplitude and phase and add coherently in forming the intensity of the scattered light. For scattering into directions other than the retroreflection direction the differential partial waves have a nonzero phase difference and very rapidly become incoherent, so that only their intensities add. Thus, the intensity of scattering into the retroreflection direction is a factor of two larger than the intensity of scattering into those other directions, because of the cross-terms that appear in the expression for the intensity in the former case. The contribution of the single-scattering processes must be subtracted in obtaining this factor of two enhancement, because it is not subject to

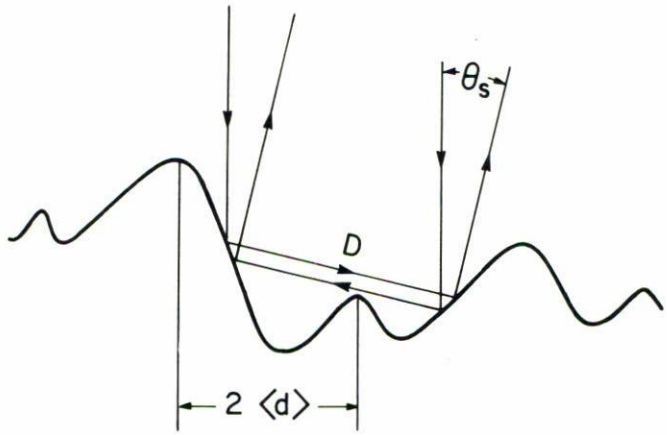

FIGURE 1. A schematic description of a light path and its time-reversed partner in a typical double-scattering event.

coherent backscattering. In practice it is found that most of the enhanced backscattering is contained in the lowest order $(n + 2)$ contribution to the mean differential reflection coefficient (drc) from the incoherent component of the scattered light [11,12].

Such a pair of scattering sequences is illustrated in the double scattering case in Fig. 1. For normal incidence the phase difference ϕ between a given light path and its time-reserved partner is proportional to $(2\pi/\lambda)\theta_s D$, where θ_s is the scattering angle, D is the distance between the first and last scattering points on the surface, and λ is the wavelength of the light. One then expects subsidiary maxima in the dependence of $\langle \partial R_{p,s}/\partial\theta_s \rangle_{\text{incoh}}$ on θ_s when the average phase shift $\langle\phi\rangle$ is multiple of 2π, that is at angles of observation given by

$$\theta_s = \frac{n\lambda}{\langle D \rangle}, \tag{2.13}$$

where n is the order of interference. Similarly, we expect subsidiary minima when the average phase shift $\langle\phi\rangle$ is a half-odd integer multiple of 2π, that is at angles of observation given by

$$\theta_s = \left(n + \frac{1}{2}\right) \frac{\lambda}{\langle D \rangle}. \tag{2.14}$$

The last result suggests that the angular width of the enhanced backscattering peak is

$$\Delta\theta_s = \frac{\lambda}{\langle D \rangle}. \tag{2.15}$$

Since the average value of D for the shortest scattering sequence (double scattering) is the mean distance between two scattering events, i.e. the elastic mean free path ℓ of the

light interacting with the surface, the angular width of the enhanced backscattering peak is expected to be of the order of λ/ℓ.

There is no good way at the present time to calculate $\langle D \rangle$ or ℓ, although ray tracing calculations might be helpful here. However, it was suggested in Ref. [11] on physical grounds that in scattering from large amplitude, highly reflecting, random surfaces, a good estimate of ℓ should be given by the mean distance between consecutive peaks and valleys on the surface, $\langle d \rangle$. A method for calculating this distance has been presented in Ref. [52]. (In the case of scattering from weakly corrugated surfaces, where it is the multiple scattering of surface electromagnetic waves that is believed to be the dominant mechanism responsible for enhanced backscattering, it is the mean free path of the surface electromagnetic wave, due to ohmic losses and radiation damping, that determines the width of the enhanced backscattering peak [2].)

One of the striking features of theoretical [8,11] and experimental results [25,26,28,30] for the angular distribution of the intensity of the incoherent component of normally incident light scattered from a random grating is the presence of at most one pair of subsidiary maxima, corresponding to $n = \pm 1$, on both sides of the enhanced backscattering peak. The absence of higher order subsidiary maxima has been explained earlier [11] by the observation that the standard deviation σ_ϕ of the phase difference ϕ at an angle of observation given by Eq. (3.13) is $2\pi|n|\sigma_D/\langle D \rangle$, where σ_D is the standard deviation of D. The theoretical and experimental results thus suggest that for $n = 2\sigma_\phi$ is sufficiently large to destroy all interference effects.

In the remainder of this section we present the results of several calculations intended to test these explanations.

2.1.1 Dependence of enhanced backscattering on the form of the surface height correlation function [53]

We have argued earlier that the enhanced backscattering of light from a moderately rough, strongly reflecting, random surface is a multiple-scattering effect. If this is indeed the case, we should expect to see it from any random surface that can scatter light multiply. Such properties of the surface profile function as its correlation function $W(|x_1|)$, the statistics it obeys, and whether it is a stationary stochastic process or not, should then play subsidiary roles in the formation of the enhanced backscattering peak and other features of the angular distribution of the intensity of the incoherent component of the scattered light. In this and the following two sections of this article we explore the validity of these expectations in the context of the scattering of p- and s-polarized light from one-dimensional, random, metal surfaces.

To begin, we should try to define more precisely what we mean by a surface that scatters light multiply. At the present time there does not seem to be any generally accepted criterion that allows one to decide whether a given (single-scale) random surface, characterized by an rms height δ and a transverse correlation length a, will multiply scatter light of wavelength λ whose angle of incidence is θ_0. A way of proceeding to obtain such a criterion is to consider what is meant by a surface that does not scatter light multiply. Now, a surface for which the Kirchhoff approximation is valid is one that does not scatter light

multiply, since the Kirchhoff approximation is a single-scattering approximation. This suggests that if we know the limits of applicability of the Kirchhoff approximation we can make at least a crude estimate of when a surface can scatter light multiply. The Kirchhoff approximation is certainly expected to be valid when $\lambda \ll \rho$, where $\rho = \langle(\zeta''(x_1))^2\rangle^{-1/2}$ is the rms radius of curvature of the surface at each point. When this condition, which is independent of the angle of incidence, is satisfied, the incident light sees a surface that locally is nearly planar, and this is the condition which ensures that a single-scattering approximation is valid. If we assume for the surface height correlation function $W(|x_1|)$ the Gaussian form $W(|x_1|) = \exp(-x_1^2/a^2)$, it is straightforward to show that $\rho = (a^2/\delta)/\sqrt{12}$ in this case. The criterion for the validity of the Kirchhoff approximation given above thus becomes $\lambda \ll (a^2/\delta)\sqrt{12}$. This results can be rewritten as $\delta/a \ll (a/\lambda)/\sqrt{12}$. Provided that $\lambda/a \gtrsim 1.44$, this criterion is consistent with the criterion $\delta/a < 0.2\cos\theta_0$ proposed by Nieto-Vesperinas and Soto-Crespo [5] on the basis of numerical simulation studies of the scattering of p- and s-polarized light from random gratings on perfect conductors, characterized by the same Gaussian form for $W(|x_1|)$. More stringent criteria for the validity of the Kirchhoff approximation that depend on the wavelength λ of the incident light as well as on δ, a, and θ_0 have been presented in graphical form by Soto-Crespo and Nieto-Vesperinas [54], but the global inequality $\delta/a \ll (a/\lambda)/\sqrt{12}$ remains valid in comparison with these criteria. Therefore, on the assumption that the breakdown of the Kirchhoff approximation signals the beginning of the regime of parameter values characterizing the random surface and the incident light within which the surface can scatter light multiply, the criterion that defines this regime becomes $\lambda > \rho$, which translates into $\lambda/a > (a/\delta)/\sqrt{12}$ for the Gaussian form for $W(|x_1|)$. The results presented below will be seen to be roughly consistent with this admittedly crude criterion, *i.e.*, to within an order of magnitude.

In this section we examine some aspects of the way in which the enhanced backscattering from surfaces that scatter light multiply depends on the form of the surface height correlation function $W(|x_1|)$, and on the relation between the wavelength of the incident light and the parameters characterizing the surface roughness through $W(|x_1|)$.

We first present results of numerical simulations of the scattering of p- and s-polarized light from random metallic gratings, for four different forms of the surface height correlation function $W(|x_1|)$. The computational method used is the one described in the preceding section. The plane of incidence (the x_1x_3-plane is perpendicular to the generators of these gratings. The four forms for $W(|x_1|)$ that we consider together with the corresponding surface structure factors are:

$$a)\ W(|x_1|) = a^2/(x_1^2 + a^2) \tag{2.16a}$$

$$g(|Q|) = \pi a \exp(-|Q|a), \tag{2.16b}$$

$$b)\ W(|x_1|) = \exp(-x_1^2/a^2) \tag{2.17a}$$

$$g(|Q|) = \pi^{1/2} a \exp(-Q^2a^2/4), \tag{2.17b}$$

$$c)\ W(|x_1|) = \sin^2(\pi x_1/2a)/(\pi x_1/2a)^2 \tag{2.18a}$$

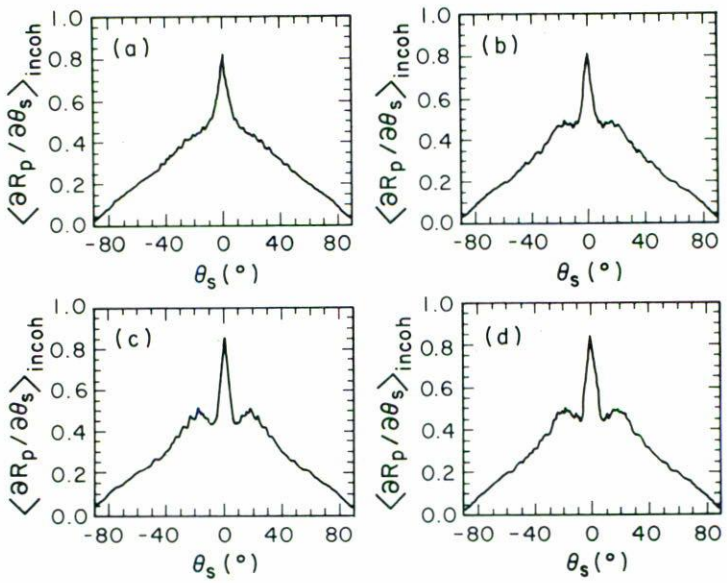

FIGURE 2. The contribution of the mean differential reflection coefficient from the incoherent component of the scattered light for the scattering of p-polarized light of wavelength $\lambda = 0.6127$ μm incident normally on a random silver grating. $\epsilon(\omega) = -17.2 + i0.498$, $a = 2$ μm, $g = 6.4$ μm, $L = 25.6$ μm, $N = 300$, $N_p = 1000$. (a) Eq. (2.16), $\delta = 1.2$ μm; (b) Eq. (2.17), $\delta = 1.2$ μm; (c) Eq. (2.18), $\delta = 1.3232$ μm; (d) Eq. (2.19), $\delta = 0.936$ μm (Ref. [53]).

$$g(|Q|) = 2a[1 - (|Q|a/\pi)]\theta(\pi - |Q|a), \tag{2.18b}$$

$$d)\ W(|x_1|) = \sin(\pi x_1/a)/(\pi x_1/a) \tag{2.19a}$$

$$g(|Q|) = a\theta(\pi - |Q|a), \tag{2.19b}$$

where $\theta(x)$ is the Heaviside unit step function. Since each of these surface height, correlation functions depends on only one characteristic length along the x_1-axis, viz. a, we can call them single-scale surfaces. We have presented these four forms for $W(|x_1|)$ in the order of increasing rate of decay to zero of their power spectra as $|Q| \to \infty$.

The mean distance $\langle d \rangle$ between consecutive peaks and valleys on each of the surfaces defined by Eqs. (2.16)-(2.19), calculated by the methods of Ref. [52], is $\langle d \rangle = 0.9080a$, $1.2837a$, $1.5823a$, and $1.2882a$, respectively. The standard deviation of this distance, $\sigma_d = [\langle d^2 \rangle - \langle d \rangle^2]^{1/2}$, for each of these four surfaces, calculated by the same methods, is $\sigma_d/\langle d \rangle = 0.60, 0.49, 0.43$, and 0.36, respectively. Consequently, it appears as if $\sigma_d/\langle d \rangle$ is smaller the more rapidly $g(|Q|)$ tends to zero as $|Q| \to \infty$.

In Fig. 2 we present the contribution to the mean differential reflection coefficient from the incoherent component of the scattered light, as a function of the scattering angle θ_s, for p-polarized light of wavelength $\lambda = 0.6127$ μm incident normally on a random grating ruled on a silver surface, when the roughness is characterized by the four correlation functions (2.16)-(2.19). In each case the characteristic length a has been chosen to be

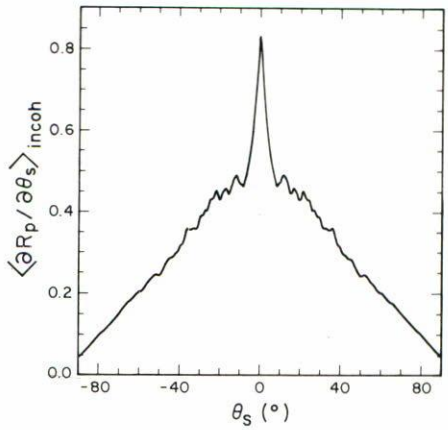

FIGURE 3. The contribution to the mean differential reflection coefficient from the incoherent component of the scattered light for the scattering of p-polarized light of wavelength $\lambda = 0.6127$ μm incident normally on a random silver grating, whose surface height correlation function is given by Eq. (2.16a). $\epsilon(\omega) = -17.2 + i0.498$, $a = 2.5$ μm, $\delta = 1.5$ μm, $g = 6.4$ μm, $L = 25.6$ μm, $N = 300$, $N_p = 1000$ (Ref. [53]).

2 μm, so that from the results given above the mean distance between consecutive peaks and valleys on the surface, $\langle d \rangle$, is also close to 2 μm. For each form of the surface height correlation function $W(|x_1|)$ the value of the rms height, δ of the surface has been chosen in such a way that the rms slope of the surface is 0.8485. For each form of $W(|x_1|)$ a well-defined peak in the retroreflection direction is present. The angular width of the peak is given very closely by $\lambda/\langle d \rangle$. In the case of scattering from the surfaces defined by the correlation functions (2.17)-(2.19) well-defined subsidiary maxima are observed at scattering angles θ_s that are quite close to $\theta_s = \pm\lambda/\langle d \rangle$. No such subsidiary maxima are present in the result for scattering from the surface defined by the Lorentzian surface height correlation function, Eq. (2.16a). However, if in this case the characteristic length a is increased to $a = 2.5$ μm, while δ is increased to $\delta = 1.5$ μm, so that the rms slope of the surface remains 0.8485, subsidiary maxima are present on both sides of the enhanced backscattering peak (Fig. 3).

The criterion $\lambda > \rho$ given above as defining the conditions under which the surface scatters light multiply, takes the following form for each of the form of $W(|x_1|)$ given by Eqs. (2.16)-(2.19); (a) $\lambda/a > (a/\delta)/\sqrt{24}$; (b) $\lambda/a > (a/\delta)/\sqrt{12}$; (c) $\lambda/a > (a\delta)(\sqrt{15}/\pi^2)$; (d) $\lambda/a > (a/\delta)(\sqrt{5}/\pi^2)$. The left hand side of each inequality is fixed at $\lambda/a = 0.3064$ in each case; the right hand sides have the values of 0.3402, 0.4811, 0.5931, 0.4843, respectively. These results and the fact that each of the forms of $W(|x_1|)$ assumed gives rise to enhanced backscattering for the values of λ, δ, and a adopted, indicate that the suggested criterion defining the conditions under which a given random surface scatters light multiply can be sharpened.

In Fig. 4 we present the contribution to the mean differential reflection coefficient from the incoherent component of the scattered light for the scattering of s-polarized light of wavelength $\lambda = 0.6127$ μm incident normally on a random grating ruled on a silver

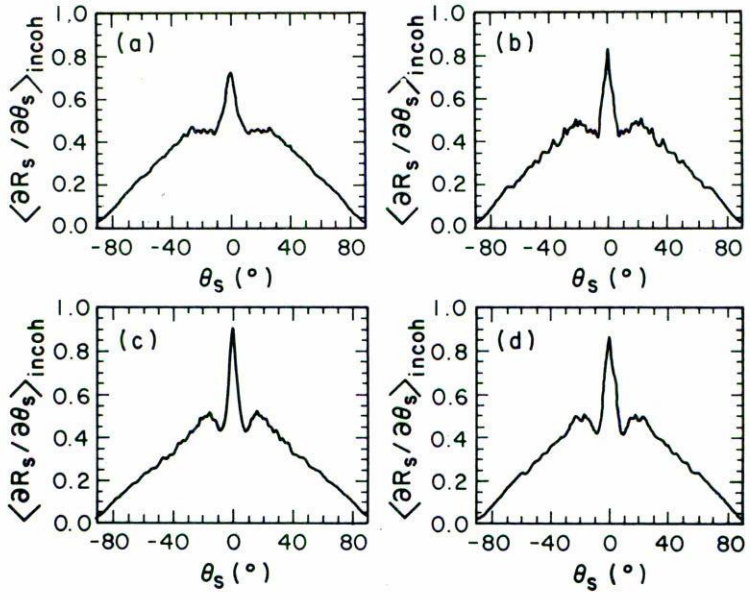

FIGURE 4. The same as Fig. 2, but for s-polarized light (Ref. [53]).

surface, whose roughness is characterized by the four surface height correlation functions (2.16)-(2.19) with the same roughness parameters as were used in plotting Fig. 2. The results are very similar to those obtained for the scattering of p-polarized light, except that the subsidiary maxima are more pronounced in s-polarization than in p-polarization. This qualitative feature is present in our earlier results [12].

The absence of subsidiary maxima corresponding to $n = \pm 2$ in the results presented in Figs. 2-4 suggests that a value of $\sigma_d/\langle d \rangle \geq 0.36$ is large enough to destroy the interference effects that would otherwise give rise to them.

We have argued earlier that the angular width of the enhanced backscattering peak should be given closely by $\lambda/\langle d \rangle$. It is of interest to explore if this is the case or not. Since for the four single-scale surfaces defined by Eqs. (2.16)-(2.19) there are only small qualitative differences among the mean differential reflection coefficients obtained through their adoption, we assume here the Gaussian surface height correlation function (2.17a), and study how the angular width of the enhanced backscattering peak changes as we increase the ratio λ/a. From the relation $\langle d \rangle = 1.2837a$, which obtains for this choice of $W(|x_1|)$, we see that this is essentially the same as changing the ratio $\lambda/\langle d \rangle$ for this surface.

In Fig. 5 we plot the contribution to the mean differential reflection coefficient from the incoherent component of p-polarized light scattered from a random grating on a silver surface. The surface profile function $\zeta(x_1)$ is assumed to be a stationary Gaussian process, with a surface height correlation function given by Eq. (2.17a). The light is incident normally. Its wavelength is $\lambda = 0.6127$ μm. The transverse correlation length a is decreased systematically so that the ratio λ/a increases from $\lambda/a = 0.0766$ to $\lambda/a = 1.225$. At the same time the value of δ is decreased, so that the ratio δ/a remains equal to 0.6.

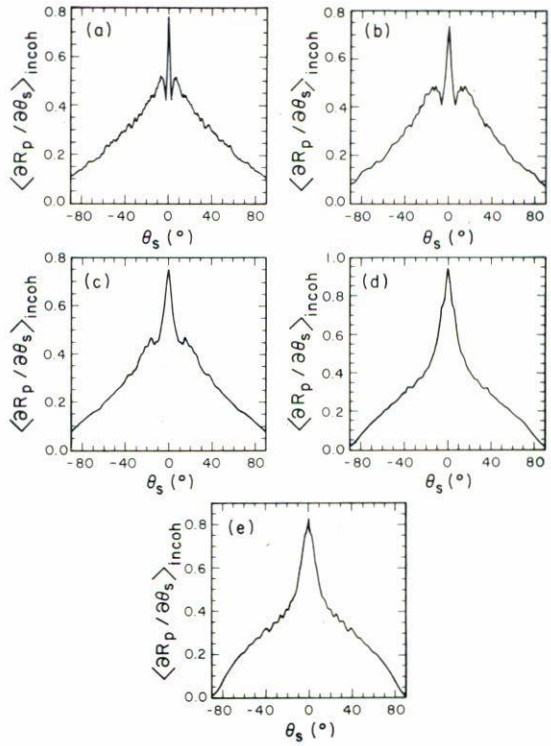

FIGURE 5. The contribution to the mean differential reflection coefficient from the incoherent component of the scattered light for the scattering of p-polarized light of wavelength $\lambda = 0.6127$ μm incident normally on a random silver grating, whose surface height correlation function is given by Eq. (2.17a). $\epsilon(\omega) = 17.2 + i0.498$, $\delta/a = 0.6$, $g = 6.4$ μm, $L = 25.6$ μm, $N = 300$, $N_p = 1000$. (a) $\lambda/a = 0.0766$; (b) $\lambda/a = 0.153$; (c) $\lambda/a = 0.306$; (d) $\lambda/a = 0.613$; (e) $\lambda/a = 1.225$ (Ref. [53]).

We see from these results that for the smallest value of λ/a, narrow enhanced backscattering peak is present in $\langle \partial R_p/\partial \theta_s \rangle_{\text{incoh}}$, together with two very well defined subsidiary maxima on either side of the main peak. As λ/a increases the width of the enhanced backscattering peak also increases, the positions of the subsidiary maxima move to larger values of $|\theta_s|$, and the subsidiary maxima themselves become progressively weaker. By the time the value of λ/a has increased to 0.613 well-defined subsidiary maxima have disappeared, and the backscattering peak is hardly distinguishable from the background.

The washing out of the subsidiary maxima as λ/a is increased that is observed in Fig. 5 is due to the fact that as λ becomes comparable with and larger than a the scattering becomes insensitive to surface perturbation on this length scale.

In Fig. 6 we use the results presented in Fig. 5, and others not shown, to plot $\Delta\theta_s$, the angular width of the enhanced backscattering peak, as a function of $(\lambda/a)(180/\pi)$, and see that for values of $(\lambda/a)(180/\pi)$ up to 45° there is a linear dependence of $\Delta\theta_s$ on this quantity with a slope close to unity. The deviations from linearity in this dependence for larger values of $(\lambda/a)(180/\pi)$ are due in large part to the difficulty of determining the width of the backscattering peak once the subsidiary maxima have been washed out.

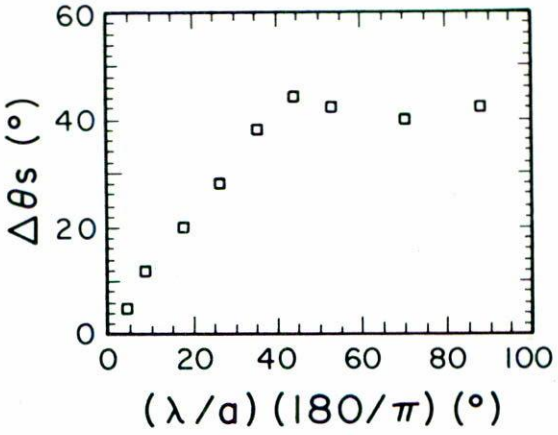

FIGURE 6. A plot of the angular width of the enhanced backscattering peak, $\Delta\theta_s$, as a function of $(\lambda/a)(180/\pi)$, obtained from the results presented in Fig. 5 (Ref. [53]).

The fact that enhanced backscattering is observed in the results presented in Figs. 5a-5c, although the inequality $\lambda/a > (a/\delta)/\sqrt{12}$ is not satisfied in these cases, is additional evidence that the criterion $\lambda > \rho$ for deciding whether a given surface scatters multiply can be sharpened. A better criterion appears to be $\lambda > (\rho/10)$.

2.1.2 Band-limited fractal surfaces [53]

An interesting class of one-dimensional random surfaces is defined by the surface structure factor

$$g(|Q|) = \frac{\theta(Q_0 - |Q|)}{\tan^{-1} Q_0 a} \frac{\pi a}{1 + Q^2 a^2}, \tag{2.20a}$$

where $\theta(x)$ is the Heaviside limit step function. The surface height correlation function that corresponds to it is

$$W(|x_1|) = \frac{a}{\tan^{-1} Q_0 a} \int_0^{Q_0} dQ \, \frac{\cos Q x_1}{1 + Q^2 a^2}, \tag{2.20b}$$

which can only be evaluated numerically. The presence of the characteristic length Q_0^{-1} in these forms for the surface height correlation function and its corresponding power spectrum, in addition to the characteristic length a, means that in contrast to the single-scale surfaces defined by Eqs. (2.16)-(2.19), the surface defined by Eq. (2.20a) or (2.20b) is not a single-scale surface. In the limit as the cutoff wavenumber Q_0 tends infinity $g(|Q|)$ approaches $2a/(1 + Q^2a^2)$ and $W(|x_1|)$ approaches $\exp(-|x_1|/a)$. By the method of Ref. [55] it can be shown that in this limit the surface defined by these forms for $g(|Q|)$ or $W(|x_1|)$ is a fractal surface with the fractal dimension $D = 1.5$. Thus, although the

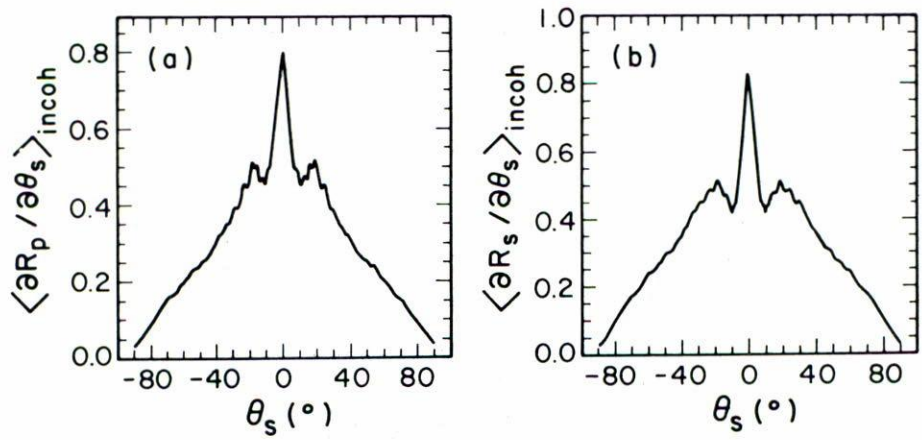

FIGURE 7. The contribution to the mean differential reflection coefficient from the incoherent component of the scattered light in the scattering of light of wavelength $\lambda = 0.6127$ μm incident normally on a random silver grating whose surface height correlation function is given by Eq. (2.20*b*). $\epsilon(\omega) = -17.2 + i0.498$, $a = 2\mu$m, $\delta = 1.1766$ μm, and $Q_0 a = 4.102$. $g = 6.4$ μm, $L = 25.6$ μm, $N = 300$, $N_p = 1000$. (a) p-polarization; (b) s-polarization (Ref. [53]).

surface defined by Eqs. (2.20) has the dimension $D = 1$ for any finite value of Q_0, it may be termed a band-limited fractal surface.

A good analytic estimate of the mean distance $\langle d \rangle$ between consecutive peaks and valleys on a random surface is provided by $\lim_{L\to\infty} L/\langle N_L \rangle$, where N_L is the number of zeros of $\zeta'(x_1)$ in a segment of length L of the x_1-axis [52]. For the surface defined by Eqs. (2.20) this estimate yields the result that

$$\langle d \rangle = \pi a \frac{(aQ_0 - \tan^{-1} aQ_0)^{1/2}}{(\frac{1}{3}a^3Q_0^3 - aQ_0 + \tan^{-1} aQ_0)^{1/2}}, \tag{2.21}$$

which has the limiting forms $\langle d \rangle = (5/3)^{1/2}\pi a/(aQ_0)$ as $aQ_0 \to 0$ and $\langle d \rangle = \sqrt{3}\pi a/aQ_0$ as $aQ_0 \to \infty$. Therefore, for a fixed value of a in the limit as $aQ_0 \to \infty$, and the surface defined by Eqs. (2.20) becomes a fractal surface, the mean distance between consecutive peaks and valleys on the surface goes to zero. In this limit physical optics has no place in the theory of scattering from such a surface.

The contribution to the mean differential reflection coefficient from the incoherent component of p- or s-polarized light scattered from the random surfaces defined by Eq. (2.20*a*) or (2.20*b*) resembles that for the scattering of light of both polarizations from the random, single-scale surfaces presented in Figs. 2 and 4, provided $\lambda/\langle d \rangle$ is of the order of 0.3 or smaller. This is illustrated in Fig. 7 in which we plot the mean drc for the scattering of p-polarized (Fig. 7a) and s-polarized (Fig. 7b) light from such a surface on a silver substrate. The wavelength of the incident light is 6127 Å, and the angle of incidence is $\theta_0 = 0°$. The roughness of the surface is characterized by the parameters $\delta = 1.1766$ μm, $a = 2$ μm, and $Q_0 a = 4.102$. The rms slope of the surface is 0.8485. The mean distance between consecutive peaks and valleys on this surface $\langle d \rangle$, calculated

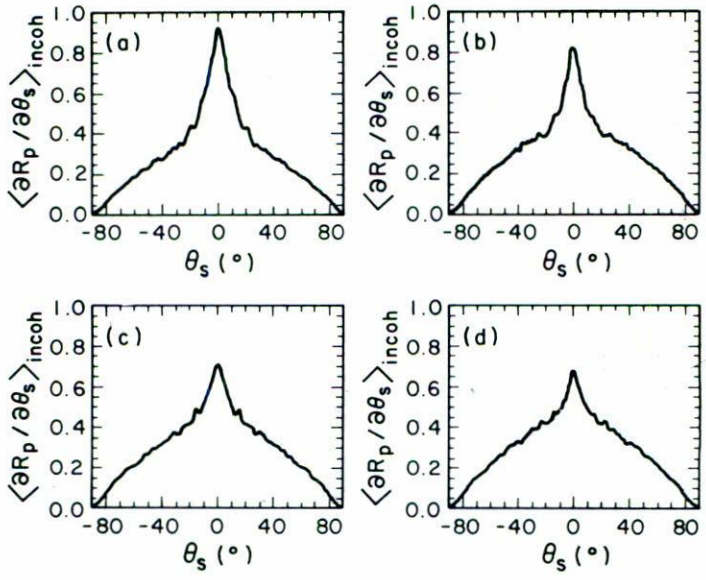

FIGURE 8. The contribution to the mean differential reflection coefficient from the incoherent component of the scattered light for the scattering of p-polarized light of wavelength $\lambda = 0.6127$ μm incident normally on a random silver grating whose surface height correlation function is given by Eq. (2.20*b*). $\epsilon(\omega) = -17.2 + i0.498$, $a = 2$ μm, $g = 6.4$ μm, $L = 25.6$ μm, $N_p = 1000$. (a) $Q_0 a = 10.25$, $\delta = 0.695$ μm, $N = 300$; (b) $Q_0 a = 20.51$, $\delta = 0.480$ μm, $N = 300$; (c) $Q_0 a = 30.1$, $\delta = 0.389$ μm, $N = 300$; (d) $Q_0 a = 41.02$, $\delta = 0.336$ μm, $N = 400$ (Ref. [53]).

exactly by the method of Ref. [52], is $\langle d \rangle = 1.327a$ for this value of $Q_0 a$. We therefore have that $\lambda/\langle d \rangle = 0.2309$. For both polarizations of the incident light a well-defined peak is present in the retroreflection direction $\theta_s = 0°$. In addition, well-defined subsidiary maxima are present on both sides of this enhanced backscattering peak.

The situation rapidly changes as we increase $Q_0 a$, keeping a fixed, and decreasing δ to keep the *rms* slope of the surface fixed at 0.8485. We preface the calculations that show this with the following observation.

If it is indeed the case that the angular width of the enhanced backscattering peak is given by λ/ℓ, and that a good estimate of the mean free path ℓ for large amplitude, highly reflecting, random surfaces is provided by $\langle d \rangle$, the mean distance between consecutive peaks and valleys on the surface, then we would expect that the width of the enhanced backscattering peak calculated for the scattering of light from the band-limited fractal surface defined by the surface height correlation function (2.20) for a fixed value of a should broaden as the product aQ_0 increases indefinitely, the surface becomes more and more fractal-like, and $\langle d \rangle$ tends to zero. This, in fact, is what is observed.

In Fig. 8 we plot the contribution to the mean differential reflection coefficient from the incoherent component of the scattered light, when p-polarized light whose wavelength is $\lambda = 0.6127$ μm is incident normally on a band-limited fractal surface characterized by four values of aQ_0 that increase from 10.25 to 41.02. The values of $\lambda/\langle d \rangle$ for the surfaces used

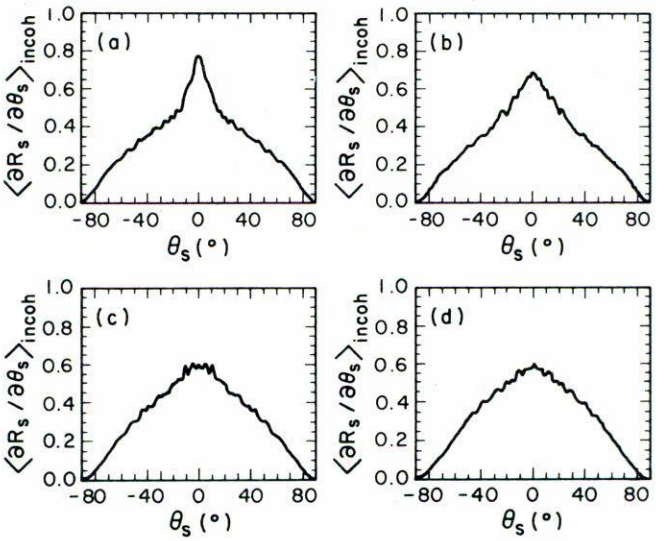

FIGURE 9. The same as Fig. 8, but for s-polarized light (Ref. [53]).

in obtaining Figs. 8a-d are 0.6163, 1.174, 1.771, and 2.357, respectively, and have been calculated by the method of Ref. [52]. The results in Figs. 8a-d should be compared with the one in Fig. 7a, for which $Q_0 a = 4.102$. We see that whereas well-defined subsidiary maxima are present in the latter result, there is essentially no evidence of such structure in the results depicted in Figs. 8a-8d. We also see that as aQ_0 is increased the enhanced backscattering peak at $\theta_s = 0°$ broadens, becomes less well-defined, and merges more and more into the background.

These effects are even more dramatically displayed in the corresponding results for the scattering of s-polarized light from the same surfaces, for which results are presented in Fig. 9. Again, although well-defined subsidiary maxima are observed in the result presented in Fig. 7b, for which $Q_0 a = 4.102$, there is no evidence for them in any of the results displayed in Figs. 9a-9d. In this case the broadening of the enhanced backscattering peak with increasing $Q_0 a$ is so rapid that already for $Q_0 a = 20.51$ the peak is almost indistinguishable from the background, and for $Q_0 a = 30.08$ and 41.02 no peak is visible. Indeed, the mean differential reflection coefficients for the latter two cases, Figs. 9c and 9d, are almost Lambertian.

The broadening of the enhanced backscattering peaks with increasing $Q_0 a$ is consistent with the corresponding decrease in $\langle d \rangle$ and the suggestion that the width of the backscattering peak is $\lambda / \langle d \rangle$. The disappearance of the subsidiary maxima as $Q_0 a$ is decreased is due to the fact that once $\langle d \rangle$ becomes sufficiently small relative to λ, the incident light cannot resolve the surface structure that is responsible for the subsidiary maxima.

2.1.3 Non-Gaussian statistics [8]

In much, if not most, of the theoretical work done to date on the scattering of light from random surfaces, and even in some of the experimental work, it has been assumed that the surface profile function $\zeta(x_1)$ (in the case of one-dimensional surfaces) is a Gaussianly distributed random variable. This is due primarily to the simplifications introduced into the theoretical work by this assumption. Scattering from non-Gaussian surfaces has been much less actively studied [8,56-63]. Yet the scattering of light from non-Gaussian surfaces deserves to be studied for several reasons. Many surfaces of practical importance do not obey Gaussian statistics, *e.g.*, a very rough sea [57] and a terrain with sharp ridges and round valleys [57]. It is also a difficult experimental problem to fabricate random surfaces that obey Gaussian statistics, although significant progress in doing so has been made recently [45,46]. At the same time methods exist for fabricating certain types of non-Gaussian surfaces [61,64]. Finally, theories based on the assumption that the surface profile function is a Gaussianly distributed random variable and a particular form for the surface height correlation function are sometimes in good agreement with experimental data. Is this because the measured surfaces were approximately Gaussian, or is it because the statistical properties of a surface profile function are not critical for its scattering properties? Until the scattering properties of non-Gaussian surfaces are know, it is not possible to give convincing answers to these questions [61].

We have studied the scattering of p- and s-polarized light from a random surface whose surface profile function is [8]

$$\zeta(x_1) = \sum_{n=-\infty}^{\infty} c_n s(x_1 - n\Delta x) \tag{2.22}$$

In this expression the $\{c_n\}$ are independent random variables with the properties

$$\begin{aligned} c_n &= 1 - p \qquad \text{with probability } p \\ &= p \qquad\quad \text{with probability } 1 - p, \end{aligned} \tag{2.23}$$

while Δx is a length that will be defined below. The function $s(x_1)$ was assumed to have the form

$$s(x_1) = A\exp(-x_1^2/R^2) \tag{2.24}$$

It is not difficult to show that the surface profile function defined by Eqs. (2.22)-(2.24) is not a Gaussianly distributed random variable [8]. It possesses the following properties:

$$\langle \zeta(x_1) \rangle = 0 \tag{2.25}$$

$$\langle \zeta(x_1)\zeta(x_1') \rangle = \left(\frac{\pi}{2}\right)^{1/2} \frac{p(1-p)}{\Delta x} A^2 R \exp\left[-\frac{x_1 - x_1')^2}{2R^2}\right] \tag{2.26}$$

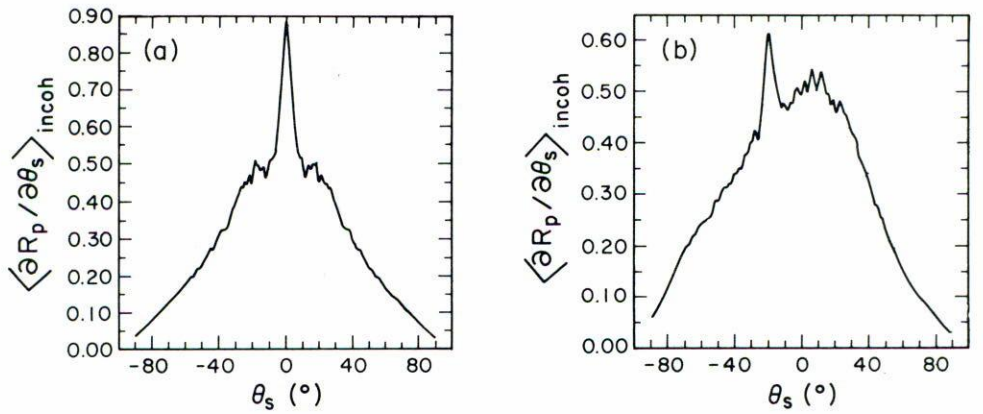

FIGURE 10. The contribution to the mean differential reflection coefficient from the incoherent component of the scattered light for the scattering of p-polarized light of wavelength $\lambda = 0.6127$ μm from a non-Gaussian random silver grating whose surface profile function is given by Eqs. (2.22)-(2.23). $\epsilon(\omega) = -17.2 + i0.498$, $\delta = 1.4142$ μm, $a = 2$ μm, and $p = 0.3$. $g = 6.4$ μm, $L = 25.6$ μm, $N = 300$, and $N_p = 930$. (a) $\theta_0 = 0°$; (b) $\theta_0 = 20°$ (Ref. [8]).

Thus, if we rewrite the last result in the form

$$\langle \zeta(x_1)\zeta(x_1') \rangle = \delta^2 \exp[-(x - 1 - x_1')^2/a_2], \tag{2.27}$$

we can make the identifications

$$\delta^2 = \left(\frac{\pi}{2}\right)^{1/2} 2\frac{p(1-p)}{\Delta x} A^2 R \tag{2.28a}$$

$$a = \sqrt{2}\, R \tag{2.28b}$$

The extra degree of freedom that the parameter p provides means that by varying p and A simultaneously we can construct a family of random surfaces having the same values of δ and a, but having qualitatively different forms. In all our calculations we have assumed that $\Delta x = a/20$.

The random surfaces generated in this way are unlikely to occur naturally. However, they can be manufactured, *e.g.*, by multiple exposure of photoresist-coated plates to a Gaussian beam.

In Fig. 10 we present our results for the scattering of p-polarized light, whose wavelength is $\lambda = 0.6127$ μm, from a silver surface of the kind we have been discussing. The dielectric constant of silver at this wavelength is $\epsilon(\omega) = -17.2 + i0.498$. The surface roughness is

characterized by the values $\delta = 1.4142$ μm and $a = 2$ μm. The value of the parameter p has been chosen to be 0.3. The angles of incidence are $\theta_0 = 0°$ (Fig. 10a) and $\theta_0 = 20°$ (Fig. 10b). A total of $N_p = 930$ different surface profiles was used in obtaining these results. For both angles of incidence the contribution to the mean differential reflection coefficient from the incoherent component of the scattered light displays a well-defined peak in the retroreflection direction. In addition, well-defined subsidiary maxima are observed on both sides of the enhanced backscattering peak in the case of the scattering of normally incident light. In fact, the result presented in Fig. 10a resembles both qualitatively and quantitatively the results for the scattering of p-polarized light from Gaussian surfaces for the same values of δ and a that have been presented in Fig. 2.

Thus, the results of this section show that, just as in the scattering of light from a Gaussian, random, metal surface, the scattering of light from a non-Gaussian random metal surface displays enhanced backscattering.

2.1.4 Non-stationary surfaces

Concluding our investigations of the kinds of random surfaces that give rise to enhanced backscattering, we explore here the consequences of relaxing the common assumption that the surface profile function is a stationary stochastic process. We do this by studying the scattering of p- and s-polarized light from random metallic gratings with large rms slopes characterized by profile functions that are even and odd functions of x_1. To obtain such surfaces we first constructed a random surface profile function $\zeta(x_1)$, obeying Gaussian statistics defined by the properties $\langle \zeta(x_1) \rangle = 0$ and $\langle \zeta(x_1)\zeta(x_1') \rangle = \delta^2 \exp(-(x_1 - x_1')^2/a^2)$, by the method described in Appendix A of Ref. [12], for x_1 in the interval $(-L/2, L/2)$. The surface profile functions of even and odd symmetry in this interval were then constructed according to $\zeta_{e,o}(x_1) = [\zeta(x_1) \pm \zeta(-x_1)]/2$, respectively. We see immediately that the surface profiles $\zeta_{e,o}(x_1)$ defined in this way are no longer stationary random processes, because the point $x_1 = 0$ is a distinguished point.

We have calculated the contribution to the mean differential reflection coefficient from the incoherent component of the scattered light, as a function of the scattering angle θ_s, for light of p-polarization incident on a silver surface whose surface is a random grating of even and odd symmetry [19]. The wavelength of the incident light was $\lambda = 6127$ Å, and the dielectric constant of silver at this wavelength is $\epsilon(\omega) = -17.2 + i0.498$. The angle of incidence was 20°. The roughness of the surfaces was characterized by the parameters $\delta = 1.4142$ μm, and $a = 2$ μm, and a total of $N_p = 1000$ different surface profiles was used in obtaining these results. In Figs. 11a and 11b we present our results for scattering from gratings of even and odd symmetry, respectively. From gratings of each symmetry type a well-defined peak is observed in $\langle \partial R_p/\partial\theta_0 \rangle_{\text{incoh}}$ in the retroreflection direction, $\theta_s = -20°$. However, in the case of scattering from the random grating of even symmetry (Fig. 11a), a second well-defined peak is observed in the specular direction, $\theta_s = 20°$. Such a peak was first observed in the results of similar calculations for perfectly conducting surfaces by Nieto-Vesperinas and Soto-Crespo [9]. We emphasize that this is a peak in the angular dependence of the intensity of the incoherent component of the scattered light. Because it enhances the peak in the specular direction in the angular dependence of the intensity of

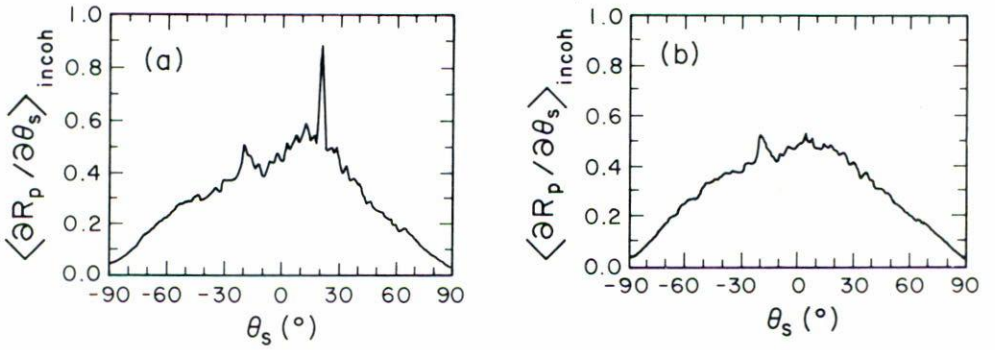

FIGURE 11. The contribution to the mean differential reflection coefficient from the incoherent component of the scattered light for the scattering of p-polarized light from a random silver grating of (a) even symmetry; (b) odd symmetry. $\theta_0 = 20°$, $\lambda = 0.6127$ μm, $\epsilon(\omega) = -17.2 + i0.498$, $\delta = 1.4142$ μm, $a = 2$ μm, $g = 6.4$ μm, $L = 25.6$ μm, $N = 300$, $N_p = 1000$ (Ref. [19]).

the coherent component of the scattered light, the existence of this peak is called specular enhancement.

However, in contrast with enhanced backscattering, which is a multiple-scattering effect, specular enhancement is already present in the Kirchhoff approximation, *i.e.*, in a single-scattering approximation. This is seen in the results presented in Fig. 12, in which we display the contribution to the mean differential reflection coefficient from p-polarized light incident on the same surface used in obtaining Fig. 11a, but ruled on a perfect conductor, for which such calculations are much simpler than for a metal. No evidence of enhanced backscattering is seen in the single scattering contribution plotted in Fig. 12b, while a well-defined specular enhancement peak is present. The pure double-scattering contribution plotted in Fig. 12c shows an enhanced backscattering peak, as well as a weak specular enhancement peak. These results are consistent with the picture of enhanced backscattering as a multiple-scattering phenomenon, and of specular enhancement as a predominantly single-scattering effect.

Specular enhancement can be understood qualitatively with following arguments. If we consider only single-scattering contributions in the scattering of light from an arbitrary random grating, the amplitude components interfering in the specular direction arise from the so-called specular points. These are points on the surface at which its slope is zero. For optically rough surfaces the random heights of the specular points have large fluctuations (compared with the wavelength λ of the incident light), and the relative phase of the farfield contributions is completely random *i.e.*, uniformly distributed in the

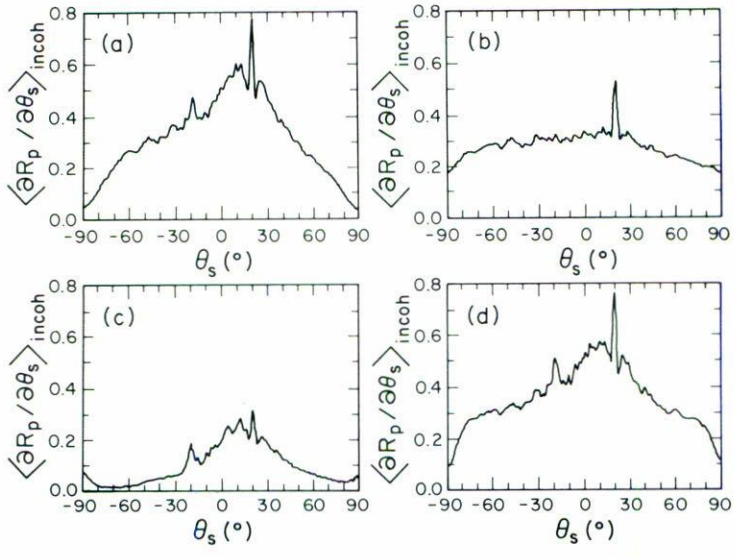

FIGURE 12. The contribution to the mean differential reflection coefficient from the incoherent component of the scattered light for the scattering of p-polarized light from a random grating of even symmetry on a perfect conductor. The parameters used in obtaining the results are those used in obtaining Fig. 11. (a) the total incoherent contribution to the mean differential reflection coefficient; (b) the contribution from the single-scattering processes; (c) the contribution from the pure double-scattering processes; (d) the contribution from the single- and double-scattering processes including the interference terms (Ref. [19]).

interval $(-\pi, \pi)$. This destroys the coherent (or specular) component of the scattered light. The situation is the same for random gratings with an odd profile. However, for random gratings with an even profile, there are pairs of contributions, arising from symmetric specular points at the same height, at x_1 and $-x_1$, which interfere constructively with a fixed, non-random, phase difference. This increases the intensity of the scattered light in the specular direction by a factor of two over that of the background.

Specular enhancement has been observed experimentally. In Fig. 13 we present the mean drc for the scattering of p-polarized light from a random grating on a gold-coated photoresist film deposited on a glass substrate. The surface is sufficiently rough that the coherent component of the scattered light is negligible. The surface consists of 150 different, contiguous segments, each of which is 200 μm long, and each of which is an even function of x_1, measured from its midpoint. The width of the incident beam is 3 cm, so that the drc plotted is equivalent to the result of averaging over 150 different realizations of a random surface. A well-defined peak is observed in the specular direction, $\theta_s = 10°$. However, no enhanced backscattering peak is observed in this figure, because the roughness parameters are such that the overwhelming contribution to the drc is due to single-scattering processes, i.e. the Kirchhoff approximation is valid.

From the results presented in this section we conclude that the enhanced backscattering of light of p-polarization from large amplitude random gratings on metal surfaces is not

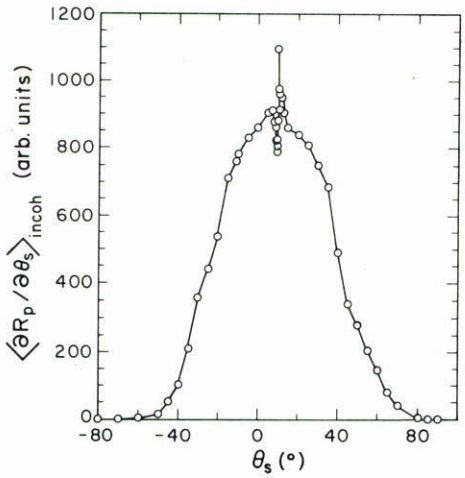

FIGURE 13. An experimental result for the contribution to the mean differential reflection coefficient from the incoherent component of the scattered light for the scattering of p-polarized light from a random grating of even symmetry on a gold-coated (d_{Au} = 500 Å) photoresist film of mean thickness $D_{ph} = 10$ μm deposited on a glass substrate of thickness $D_{gl} = 5$ mm. $\theta_0 = 10°$, $\lambda = 0.6328$ μm, $n_{ph} = 1.64$, $n_{gl} = 1.51$, $\delta = 2.3$ μm, $a = 9.5$ μm (Ref. [19]).

eliminated when the randomness of the surface is constrained by forcing the surface profile function to be an even or an odd function of x_1, nor is it eliminated by the loss of the stationarity property of the random surface. The evenness of the surface, however, gives rise to a new effect, specular enhancement, which is generally absent in the scattering from an unconstrained random surface (see, however, Ref. [8]).

2.2 The role of surface polaritons in enhanced backscattering from weakly rough surfaces

We have remarked in the Introduction that in the case of scattering from weakly rough random surfaces, for which the probability of multiple scattering of light from the surface is very small, the mechanism primarily responsible for enhanced backscattering is the following. The incident light excites a surface electromagnetic wave through the surface roughness; the surface electromagnetic wave is scattered multiply by the roughness as it propagates along the surface; it is finally converted back into light propagating away from the surface. All such scattering sequences are assumed to be uncorrelated due to the random nature of the surface. However, any such sequence and its time-reversed partner, in which the surface electromagnetic wave is scattered from the same points on the surface but in the reverse order, interfere constructively if the wave vectors of the incident and final waves are oppositely directed. These two waves have the same amplitude and phase and add coherently in forming the intensity of the scattered light. For scattering into directions other than the retroreflection direction the different partial waves have a nonzero phase difference and very rapidly become incoherent, so that only their intensities add. Thus, the intensity of scattering into the retroreflection direction is a factor of two larger than the intensity of scattering into any other direction because of the cross- terms that appear in the expression for the intensity in the former case. The contribution of the single

scattering processes must be subtracted off in obtaining this factor of two enhancement, because it is not subject to coherent backscattering. The enhanced backscattering of light due to the multiple scattering of surface electromagnetic waves by the surface roughness is sometimes described as being due to the weak localization of these surface waves by the surface roughness.

If this explanation for the enhanced backscattering of light from small-slope, randomly rough surfaces is correct, it follows that any mechanism that breaks the time-reversal invariance of the scattering system should degrade the enhanced backscattering by breaking the coherency of a given scattering sequence that contributes to backscattering with its time-reversed partner.

Alternatively, enhanced backscattering from small-slope random surfaces should be degraded, if not suppressed altogether, if the surface electromagnetic waves supported by the scattering surface can be "turned off".

In the remainder of this section we describe a way in which the time reversal symmetry of a random grating on the surface of an n-type semiconductor can be broken, and a way in which surface electromagnetic waves propagating along such a surface can be suppressed, and present the consequences for the enhanced backscattering of p-polarized light from these surfaces of each of these mechanisms.

2.2.1 Enhanced backscattering in a magnetic field [16,23]

Let us consider a semi-infinite n-type semiconductor that occupies the region $x_3 < \zeta(x_1)$, where the surface profile function $\zeta(x_1)$ has the properties described at the beginning of this section. The region $x_3 > \zeta(x_1)$ is vacuum. One way of breaking the time-reversal symmetry of this system is to apply a static magnetic field to it of magnitude H oriented along the x_2-axis, *i.e.*, parallel to the grooves of the one-dimensional random surface. The effect of the magnetic field is to make the semiconductor optically gyrotropic due to the cyclotron orbits the electrons are now forced to execute in the x_1x_3-plane. The semiconductor is now characterized by a dielectric tensor given by

$$\overleftrightarrow{\epsilon}(\omega) = \begin{pmatrix} \epsilon_1(\omega) & 0 & -i\epsilon_2(\omega) \\ & \epsilon_3(\omega) & \\ i\epsilon_2(\omega) & 0 & \epsilon_1(\omega) \end{pmatrix}, \tag{2.29}$$

where

$$\epsilon_1(\omega) = \epsilon_\infty \left(1 - \frac{\omega_p^2}{\omega} \frac{\omega + i\gamma}{\omega(\omega + i\gamma)^2 - \omega_c^2}\right), \tag{2.30a}$$

$$\epsilon_2(\omega) = \epsilon_\infty \left(\frac{\omega_p^2}{\omega} \frac{\omega_c}{\omega(\omega + i\gamma)^2 - \omega_c^2}\right), \tag{2.30b}$$

$$\epsilon_3(\omega) = \epsilon_\infty \left(1 - \frac{\omega_p^2}{\omega(\omega + i\gamma)}\right). \tag{2.30c}$$

In these expressions $\omega_p = (4\pi ne^2/\epsilon_\infty m^*)^{1/2}$ is the plasma frequency of the electrons, while $\omega_c = (eH/m^*c)$ is their cyclotron frequency, where n is the number density of the electrons, m^* is their effective mass, e is the magnitude of the electronic charge, c is the speed of light, and ϵ_∞ is a background dielectric constant. The damping constant γ is the reciprocal of the electronic relaxation time τ. If we choose the plane of incidence to be the x_1x_3-plane, the electromagnetic field in this system can still be separated into p-polarized and s-polarized components. We restrict ourselves here to p-polarized fields because it is only in this polarization that the incident light can excite surface polaritons. A consequence of the optical gyrotropy of the metal induced by the magnetic field is that the dispersion curve for p-polarized surface polaritons that exist at the semiconductor/vacuum interface in the absence of the surface roughness is nonreciprocal, *i.e.* $\omega(-k) \neq \omega(k)$. This is clearly seen from the dispersion curve for these surface polaritons, which can be written in the form [65]

$$\epsilon_v(\omega)\beta_0(k\omega) + \beta(k\omega) + k\frac{\epsilon_2(\omega)}{\epsilon_1(\omega)} = 0. \tag{2.31}$$

Here ω is the frequency and k the wavenumber of the surface polariton, $\beta_0(k\omega) = (k^2 - (\omega^2/c^2))^{1/2}$, $\beta(k\omega) = (k^2 - \epsilon_v(\omega)(\omega^2/c^2))^{1/2}$, and $\epsilon_v(\omega)$ is the Voigt dielectric constant, $\epsilon_v(\omega) = (\epsilon_1^2(\omega) - \epsilon_2^2(\omega))/\epsilon_1(\omega)$. The nonreciprocity of the solutions of Eq. (2.31) is evident from the fact that $\beta_0(k\omega)$ and $\beta(k\omega)$ are even functions of k, while the last term on the left hand side of Eq. (2.31) is an odd function of k. This nonreciprocity leads to a phase difference between a given surface polariton scattering sequence and its time-reversed partner, since the wavenumbers for forward and backward propagating surface polaritons, whose frequency is that of the incident light, are now different.

In a recent, perturbation-theoretic calculation of the enhanced backscattering of p-polarized light from a small-slope random grating ruled on the surface of a metal or an n-type semiconductor [16] it was found in both cases that the position of the peak in the angular dependence of the intensity of the incoherent component of the scattered light, which is observed in the retroreflection direction in the absence of the magnetic field, is shifted in the direction of larger scattering angles with increasing magnetic field strength. At the same time the width of the peak increases and its amplitude decreases. These results were interpreted as due to the breakdown of the coherency between the contribution to backscattering from a given light/surface polariton path and from its time-reversed partner, caused by the removal of time reversal symmetry from the scattering system by the application of an external magnetic field.

The perturbation-theoretic calculation was based on a solution of the Bethe-Salpeter equation for the two-particle Green's function in terms of which the scattered intensity is expressed. Only the contribution from the maximally-crossed diagrams was retained in the irreducible vertex function, and a pole approximation for the single-particle Green's functions entering this equation was used. Since there is some evidence [66] that in the presence of a time-reversal symmetry breaking perturbation the maximally-crossed diagrams are not the only important diagrams contributing to the irreducible vertex function, and because the pole approximation to the single-particle Green's functions emphasizes

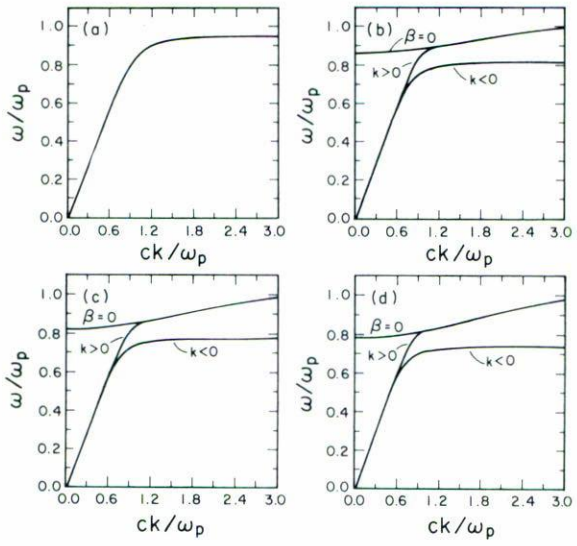

FIGURE 14. The dispersion curves for surface polaritons at a planar n-GaAs/vacuum interface for four values of an external magnetic field that is parallel to the interface and perpendicular to their direction of propagation. (a) $\omega_c/\omega_p = 0$ ($H = 0$); (b) $\omega_c/\omega_p = 0.3$ ($H = 2.46 \times 10^4$ Gauss); (c) $\omega_c/\omega_p = 0.4$ ($H = 3.28 \times 10^4$ Gauss); (d) $\omega_c/\omega_p = 0.5$ ($H = 4.10 \times 10^4$ Gauss) (Ref. [23]).

the scattering of surface polaritons at the expense of other possible contributions to enhanced backscattering, it was felt to be desirable to calculate the contribution to the mean differential reflection coefficient from the incoherent of the scattered light for the problem at hand in a nonperturbative fashion, that does not require the kinds of approximations made in the perturbative calculations of Ref. [16].

We have carried out such a calculation [23] by an extension of the numerical simulation method described in Refs. [7,11,12] to the case of an n-type semiconductor characterized by the gyrotropic dielectric tensor (2.29)-(2.30) rather than by an isotropic dielectric tensor. The semiconductor surface we have chosen to study is the (001) surface of n-GaAs. The parameters entering the dielectric tensor (2.29)-(2.30) in this case have the values $\epsilon_\infty = 10.88$, $n = 10^{18}$ cm^{-3}, and $m^* = 0.07$ m. They translate into a value of $\hbar\omega_p = 4.22 \times 10^{-2}$ eV. For the damping constant γ we used the value $\gamma = 0.09425\omega_p$, obtained from mobility data [67].

We first display, in Fig. 14, the dispersion curves for surface polaritons at a planar n-GaAs/vacuum interface, obtained by solving Eq. (2.31), for four values of ω_c/ω_p, viz. $\omega_c/\omega_p = 0$ ($H = 0$), $\omega_c/\omega_p = 0.3$ ($H = 2.46 \times 10^4$ Gauss), $\omega_c/\omega_p = 0.4$ ($H = 3.28 \times 10^4$ Gauss), and $\omega_c/\omega_p = 0.5$ ($H = 4.1 \times 10^4$ Gauss). They have been calculated with $\gamma = 0$. The values of the magnetic fields assumed in these calculations are all readily achievable experimentally. In zero external magnetic field the dispersion curve is reciprocal, and only the branch for $k > 0$ is plotted in Fig. 14a. It saturates at a frequency $\omega/\omega_p = 0.957$ as $|k| \to \infty$. For a nonzero external magnetic field the dispersion curve becomes

nonreciprocal. The branch corresponding to propagation of the surface polariton in the $-x_1$-direction ($k < 0$) exists for all negative values of the wave number k, and saturates at the frequency $\omega/\omega_p = 0.819$ when $\omega_c/\omega_p = 0.3$, at $\omega/\omega_p = 0.777$ when $\omega_c/\omega_p = 0.4$, and at $\omega/\omega_p = 0.739$ when $\omega_c/\omega_p = 0.5$. These frequencies are the solutions of the equation $1 + \epsilon_1(\omega) + \epsilon_2(\omega) = 0$, which is the form Eq. (2.31) takes in the limit as $k \to -\infty$. The branch corresponding to the propagation of the surface polariton in the $+x_1$-direction ($k > 0$) lies at higher frequencies and exists only for a limited range of wave numbers. It terminates at the point where it intersects the curve $\beta(k\omega) = 0$, which is the dispersion curve for bulk polaritons in this system. For values of k larger than the value at the point of intersection the solution of the dispersion relation (2.31) no longer describes a wave bound to the surface in the semiconductor. Thus, in the cases depicted in Figs. 14b, 14c, and 14d the dispersion curve for surface polaritons is partially nonreciprocal in the frequency ranges $0 \leq \omega/\omega_p < 0.819$, $0 \leq \omega/\omega_p < 0.777$, $0 \leq \omega/\omega_p < 0.739$, respectively, in the sense that surface polaritons with frequencies in these ranges can propagate in both the $+x_1$- and $-x_1$-directions, albeit with different wave numbers. For frequencies in the ranges $0.819 \leq \omega/\omega_p < 0.89$, $0.777 < \omega/\omega_p < 0.85$ and $0.739 < \omega/\omega_p < 0.82$, the surface polaritons whose dispersion curves are plotted in Figs. 14b, 14c, and 14d, respectively, are completely nonreciprocal, in the sense that they can now propagate only in the $+x_1$-direction; no surface polaritons can propagate in the $-x_1$-direction.

It should be noted that the plots in Figs. 14b, 14c, and 14d depict the branches of the dispersion curve in the frequency range $0 \leq \omega/\omega_p \lesssim 1$ only. There are additional branches in the frequency range $\omega/\omega_p > 1$ [65], but they are of no interest to us here.

The first set of results for the contribution to the mean differential reflection coefficient from the incoherent component of the scattered light is presented in Fig. 15, for the values of the external magnetic field used in obtaining the surface polariton dispersion curves presented in Fig. 14. The wavelength of the incident light must be chosen so that the corresponding energy $\hbar\omega$ is smaller than the value of the band gap of GaAs, viz $\hbar\omega_G = 1.35$ eV. We have assumed a value of $\lambda = 43.2$ μm ($\hbar\omega = 0.0287$ eV), corresponding to a frequency $\omega/\omega_p = 0.68$, which is below the frequencies at which the dispersion curves plotted in Fig. 14 saturate as $k \to -\infty$. The angle of incidence is $\theta_0 = 5°$. The surface roughness was characterized by the values $\delta = 3.14$ μm and $a = 15.14$ μm. A total of $N_p = 2000$ different realizations of the surface profile were used in obtaining Figs. 15a and 15b, while $N_p = 2500$ different realizations were used in obtaining Figs. 15c and 15d. In zero magnetic field a well-defined peak is seen in the retroreflection direction, $\theta_s = -5°$. This is the enhanced backscattering peak. When a magnetic field for which $\omega_c/\omega_p = 0.3$ ($H = 2.46 \times 10^4$ Gauss) is applied (Fig. 15b), the position of this peak shifts to a slightly larger angle (in magnitude), $\theta_s = 6.8°$, its amplitude decreases, and it broadens. When the magnetic field is increased to a value for which $\omega_c/\omega_p = 0.4$ ($H = 3.28 \times 10^4$ Gauss) (Fig. 15c), the position of the peak has shifted to a still larger scattering angle, $\theta_s = -7.2°$, and its amplitude has decreased still further. At a value of the magnetic field such that $\omega_c/\omega_p = 0.5$ ($H = 4.10 \times 10^4$ Gauss) the enhanced backscattering peak has almost completely disappeared (Fig. 15d). The degradation of the enhanced backscattering peak with increasing external magnetic field strength is clearly seen in the results presented in Fig. 15.

More dramatic results are obtained when we increase the frequency of the incident light, to put it in the range in which only surface polaritons propagating in the $+x_1$-

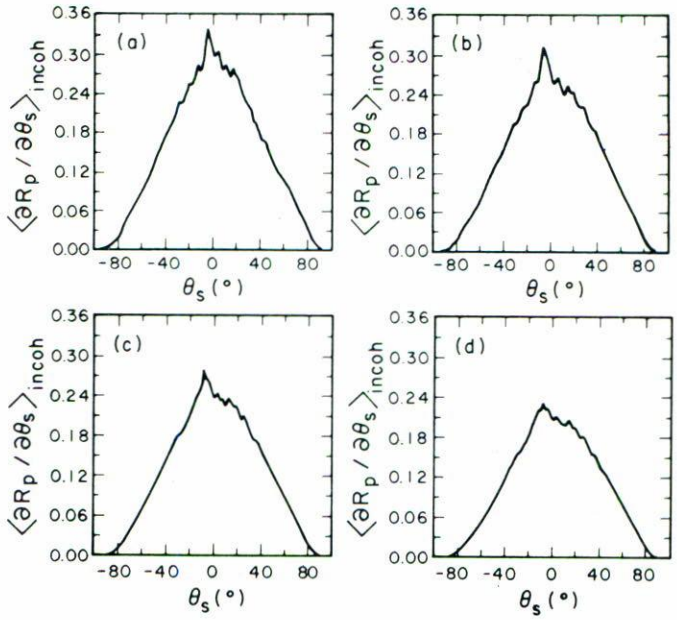

FIGURE 15. The contribution to the mean differential reflection coefficient from the incoherent component of the scattered light when p-polarized light is incident on a random n-GaAs surface characterized by $\delta = 3.14$ μm and $a = 15.14$ μm. $\lambda = 43.2$ μm ($\omega/\omega_p = 0.68$), $\theta_0 = 5°$, $g = 345.8$ μm, $L = 1388$ μm, $N = 400$. (a) $\omega_c/\omega_p = 0$ ($H = 0$), $N_p = 2000$; (b) $\omega_c/\omega_p = 0.3$ ($H = 2.46 \times 10^4$ Gauss), $N_p = 2000$; (c) $\omega_c/\omega_p = 0.4$ ($H = 3.28 \times 10^4$ Gauss), $N_p = 2500$; (d) $\omega_c/\omega_p = 0.5$ ($H = 4.1 \times 10^4$ Gauss), $N_p = 2500$ (Ref. [23]).

direction exist. In Fig. 16 we present the contribution to the mean differential reflection coefficient from the incoherent component of the scattered light when p-polarized light of wavelength $\gamma = 37.7$ μm is incident on a random n-GaAs surface characterized by the parameters $\delta = 3.14$ μm and $a = 15.14$ μm. This wavelength corresponds to a frequency of the incident light given by $\omega/\omega_p = 0.78$. The angle of incidence is $\theta_0 = 5°$. A total of $N_p = 2500$ different realizations of the surface profile was used in obtaining Fig. 16a, while $N_p = 1500$ profiles were used in obtaining Fig. 16b. In zero external magnetic field (Fig. 16a) a well-defined peak is observed in the retroreflection direction, $\theta_s = -5°$, which may be attributed to the existence of reciprocal surface polaritons at this frequency. When a magnetic field corresponding to $\omega_c/\omega_p = 0.4$ ($H = 3.28 \times 10^4$ Gauss) is applied (Fig. 16b), the frequency of the incident light falls in the range in which only forward propagating ($k > 0$) surface polaritons exist (Fig. 14c). In this case the enhanced backscattering is completely suppressed.

2.2.2 Enhanced backscattering from a randomly roughened periodic grating

In this section we show how it is possible to suppress surface polaritons within some range of frequencies on a surface that otherwise is capable of supporting them, and examine the consequences of doing so on the enhanced backscattering of light in this frequency range from a one-dimensional random surface.

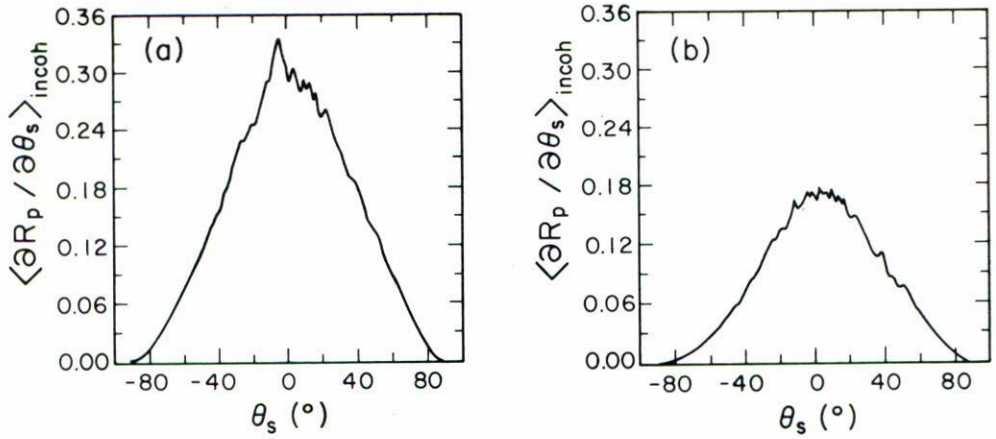

FIGURE 16. The contribution to the mean differential reflection coefficient from the incoherent component of the scattered light when p-polarized light is incident on a random n-GaAs surface characterized by $\delta = 3.14$ μm and $a = 15.14$ μm. $\lambda = 37.7$ μm ($\omega/\omega_p = 0.78$), $\theta_0 = 5°$, $g = 345.8$ μm, $L = 1383$ μm, $N = 400$. (a) $\omega_c/\omega_p = 0$ ($H = 0$), $N_p = 2500$; (b) $\omega_c/\omega_p = 0.4$ ($H = 3.28 \times 10^4$ Gauss), $N_p = 1500$ (Ref. [23]).

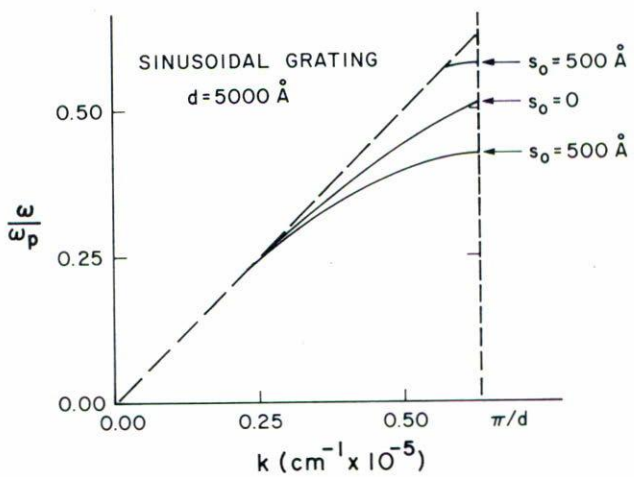

FIGURE 17. The dispersion curve for surface polaritons propagating perpendicular to the grooves and ridges of a classical grating, whose surface profile function is $\zeta(x_1) = s_0 \cos(2\pi x_1/d)$, with $s_0 = 500$ Å and $d = 5000$ Å. The substrate is a simple, free electron metal for which $\hbar\omega_p = 2$ eV. The curve labeled $s_0 = 0$ is the portion of the corresponding dispersion curve for surface polaritons at a planar metal/vacuum interface within the nonradiative region of the (ω, k)-plane (Ref. [68]).

Thus, let us consider a planar metal/vacuum interface, that supports a p-polarized surface electromagnetic wave. When a periodic, classical grating is ruled on the surface of the metal, the dispersion curve for the surface electromagnetic waves opens up gaps at wave numbers $k = n\pi/d$, where d is the period of the grating, and $n = \pm 1, \pm 2, \pm 3 \ldots$, if the Fourier coefficients $\hat{s}_0(n)$ of the periodic surface profile function $s_0(x_1)$ are nonzero for $n = \pm 1, \pm 2, \pm 3, \ldots$, respectively. This is illustrated in Fig. 17 for the case of a surface polariton propagating across a grating defined by the sinusoidal profile function $s_0(x_1) = s_0 \cos(2\pi x_1/d)$, ruled on the surface of a simple free electron metal for which $\epsilon(\omega) = 1 - (\omega_p^2/\omega^2)$ [68]. The value of $\hbar\omega_p$ has been chosen to be 2 eV while s_0 and d are 500 Å and 5000 Å, respectively. The reduced zone scheme has been used in drawing the dispersion curve inside the nonradiative region of the (ω, k)-plane. P-polarized light whose plane of incidence is perpendicular to the grooves of the grating and whose frequency falls inside the gap in this dispersion curve cannot excite surface polaritons, through the grating surface, since none exist in this frequency range. If the frequency of the incident light is lower than the frequency of the lower edge of the gap, or higher than the frequency of the higher edge of the gap, it can excite surface polaritons.

We now assume that the periodic surface profile is perturbed by random surface roughness, so that the surface profile function is now given by

$$\zeta(x_1) = s_0(x_1) + s_1(x_1), \tag{2.32}$$

where $s_1(x_1)$ is a single-valued function of x_1 and constitutes a stationary, Gaussian process defined by the properties

$$\langle s_1(x_1) \rangle = 0, \tag{2.33}$$

$$\langle s_1(x_1) s_1(x_1') \rangle = \delta^2 W(|x_1 - x_1'|). \tag{2.34}$$

The surface height correlation function $W(|x_1 - x_1'|)$ will be assumed to have the Gaussian form $\exp(-(x_1 - x_1')^2/a^2)$. If the composite surface is weakly corrugated, *i.e.*, if s_0/d and δ/a are both small, so that enhanced backscattering of p-polarized light from it should be due primarily to the surface polaritons supported by it, we should expect qualitatively different forms of the angular dependence of the intensity of the incoherent component of the scattered light, when the frequency of the incident light is in the gap in the surface polariton dispersion curve and when it is below it. In the latter case enhanced backscattering should be observed due to the existence of surface polaritons in this frequency range; in the former case enhanced backscattering should be strongly suppressed due to the absence of surface polaritons.[1]

[1]Strictly speaking, when random roughness is superimposed on the periodic corrugations of the metal surface, we expect that the density of surface polariton states will not be identically zero in the frequency range of the gap, but will be nonzero due to tails from the bands of surface polariton states for frequencies above and below the band gap that are allowed in the absence of the random roughness. Nevertheless, this nonzero density of states in the region of the gap is expected to be very small for frequencies well-removed from the band edges in the presence of weak random roughness.

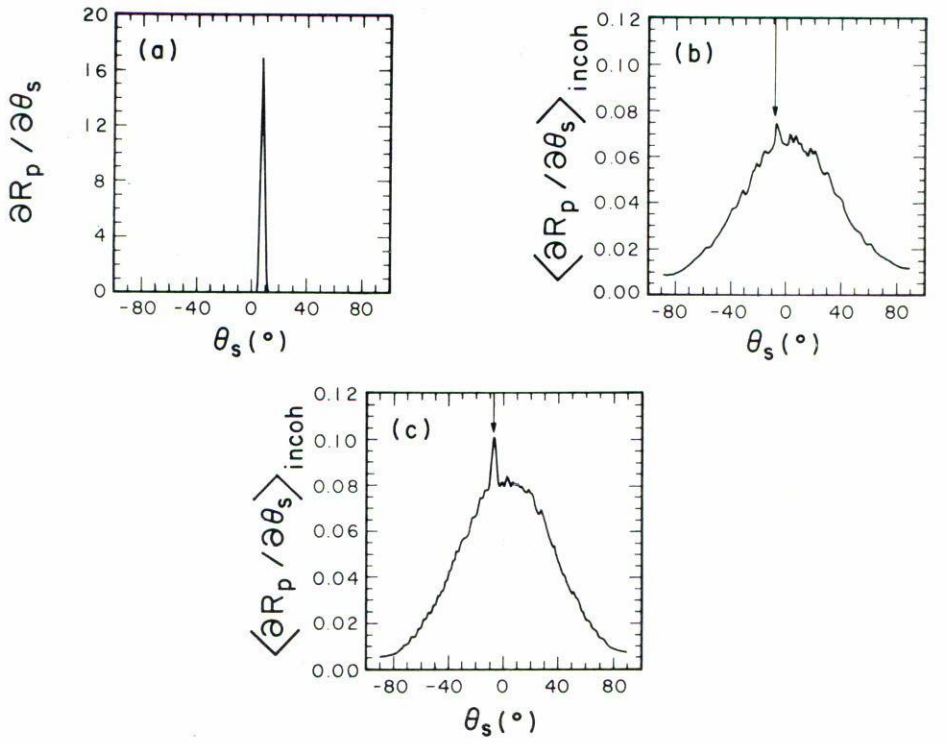

FIGURE 18. (a) The differential reflection coefficient for the scattering of p-polarized light from a sinusoidal grating defined by the profile function $s_0(x_1) = s_0 \cos(2\pi x_1/d)$, with $s_0 = 500$ Å and $d = 5000$ Å, ruled on the surface of a free electric metal ($\hbar\omega_p = 2$ eV). $\theta_0 = 7.4°$, $\lambda = 1.6102$ μm ($\omega/\omega_p = 0.385$), $\epsilon(\omega) = -5.7$. $g = 11.32$ μm, $L = 60$ μm, $N = 590$. (b) The contribution to the mean differential reflection coefficient from the incoherent component of the scattered light when p-polarized light is incident on a random grating characterized by the parameters $\delta = 400$ Å and $a = 6000$ Å, ruled on the surface of a free electron metal ($\hbar\omega_p = 2$ eV). $\theta_0 = 7.4°$, $\lambda = 1.6102$ μm ($\omega/\omega_p = 0.385$), $\epsilon(\omega) = -5.7$. $g = 11.25$ μm, $L = 45$ μm, $N = 300$, $N_p = 1000$. (c) The contribution to the mean differential reflection coefficient from the incoherent component of the scattered light when p-polarized light is incident on a surface whose profile function contains both the periodic and random components used in obtaining (a) and (b).

We have carried out numerical simulations of the scattering of p-polarized light from such a composite surface ruled on a simple free electron metal. The value of the plasma frequency of the metal was assumed to be defined by $\hbar\omega_p = 2$ eV. The values of s_0 and d characterizing the periodic contribution to the surface profile function $s_0(x_1)$ were chosen to be 500 Å and 5000 Å, respectively, *i.e.*, they were chosen to have the values used in calculating Fig. 17. The values of δ and a characterizing the random contribution $s_1(x_1)$ to the surface profile function were taken to be 400 Å and 6000 Å, respectively. A total of $N_p = 1000$ realizations of the surface was used in each of the calculations in which $s_1(x_1)$ was nonzero.

In Fig. 18 we have plotted the differential reflection coefficient for the scattering of light from this composite surface when the frequency of the light is $\omega/\omega_p = 0.385$ ($\lambda =$

1.6102 μm). This frequency is below the frequency of the lower edge of the band gap in Fig. 17, so that surface polaritons exist on this surface in the presence of the periodic grating ruled on it as well as in the absence of the grating. The value of the dielectric constant of the metal at this frequency is $\epsilon(\omega) = -5.7$ The angle of incidence is $\theta_0 = 7.4°$. Under these conditions there is only a single diffracted beam when the surface profile function is the periodic function $s_0(x_1)$, viz. the specular beam. The nonzero width of the corresponding peak in the differential reflection coefficient, plotted in Fig. 18a, is due to the finite width of the incident beam. In Fig. 18b we plot the contribution to the mean differential reflection coefficient from the incoherent component of the scattered light when the surface profile function is that of the random grating alone, $\zeta(x_1) = s_1(x_1)$. A well-defined peak is observed in the mean differential reflection coefficient when the scattering angle corresponds to the retroreflection direction, $\theta_s = -7.4°$ which is indicated by the arrow in this figure. In Fig. 18c we present the contribution to the mean differential reflection coefficient from the incoherent component of the scattered light when the surface profile function contains both the periodic and random components, $\zeta(x_1) = s_0(x_1) + s_1(x_1)$. A well-defined enhanced backscattering peak is observed in this case as well. Indeed, the peak is more pronounced in the presence of both the periodic and random corrugations of the surface than when only the random corrugations are present.

When the frequency of the incident light is increased to $\omega/\omega_p = 0.46$ ($\lambda = 1.3476$ μm), it now lies well inside the gap of the surface polariton dispersion curve depicted in Fig. 17. At his frequency surface polaritons cannot exist on the metal surface in the presence of the periodic grating ruled on it. Although they do exist on it in the absence of the periodic grating. The value of the dielectric constant of the metal at this frequency is $\epsilon(\omega) = -3.7$. The angle of incidence is now $\theta_0 = 6.2°$. Under these conditions there is again only a single diffracted beam, the specular beam, in the differential reflection coefficient when the surface profile function is the periodic function $s_0(x_1)$. This is depicted in the differential reflection coefficient plotted in Fig. 19a. In Fig. 19b we have plotted the contribution to the mean differential reflection coefficient from the incoherent component of the scattered light when the surface profile function is that of the random grating alone, $\zeta(x_1) = s_1(x_1)$. A well defined peak in the retroreflection direction (denoted by the arrow in this figure) is seen in the mean differential reflection coefficient. However, when the surface profile function contains both the periodic and random components, $\zeta(x_1) = s_0(x_1) + s_1(x_1)$, tis enhanced backscattering peak is strongly suppressed (Fig. 19c).

Thus, the results presented in Figs. 18 and 19 demonstrate a strong correlation between the presence or absence of enhanced backscattering in the scattering of light from a weakly corrugated random surface, and the presence or absence of surface polaritons on that surface at the frequency of the incident light.

2.3 Enhanced backscattering from dielectric films

Not all of the interesting manifestations of weak localization in the interaction of light with one-dimensional random surfaces are observed in reflection from semi-infinite media. In this section we explore theoretically and experimentally several additional consequences of the finite thickness of a dielectric medium for the reflection of light from it when the illuminated surface is a one-dimensional random surface, while the back surface is planar.

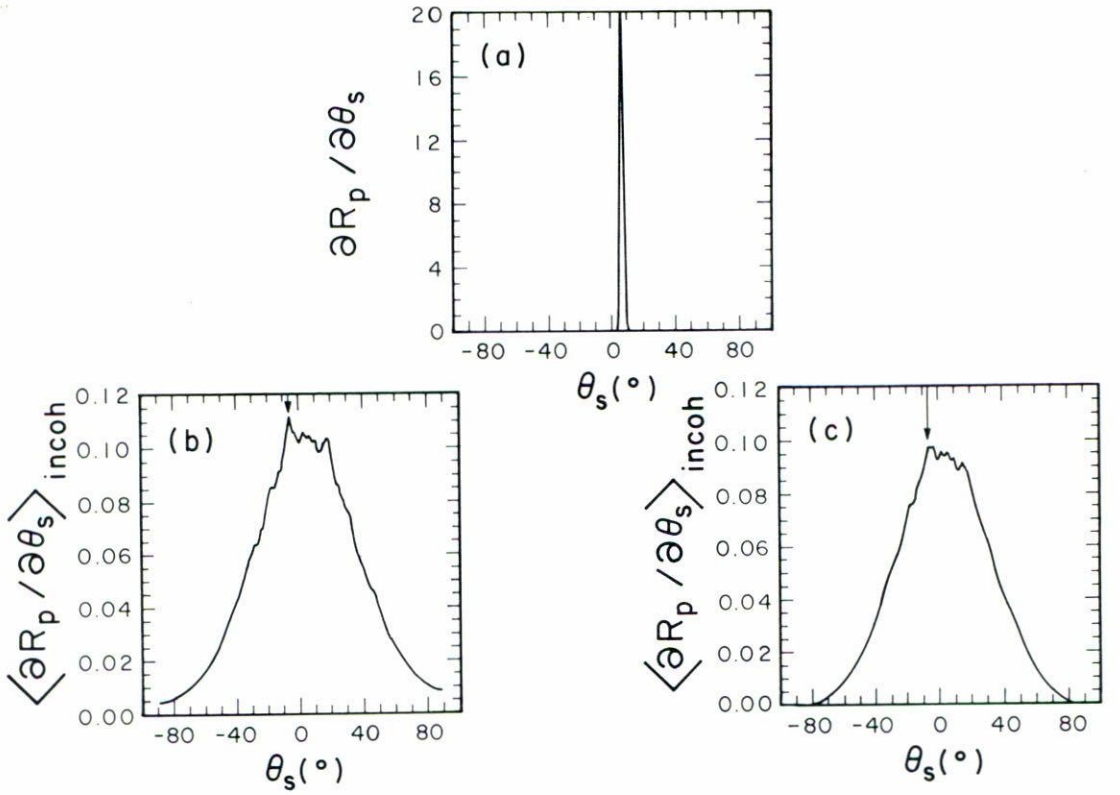

FIGURE 19. The same as Fig. 18, except that $\theta_0 = 6.2°$, $\lambda = 1.3467$ μm ($\omega/\omega_p = 0.46$), $\epsilon(\omega) = -3.7$, $N_p = 2000$.

It will be found that several effects occur in such structures that are absent in their semi-infinite counterparts.

2.3.1 Enhanced backscattering from a dielectric film on a reflecting surface [15]

In a recent series of papers Jakeman and his colleagues showed that light scattered from a deep random phase screen placed in front of a mirror displays a strong increase in its intensity in the backscattering direction. [69-71] These results suggest that it would be of interest to study the scattering of p- and s-polarized light from a structure that consists of a film of a nearly transparent dielectric of average thickness d deposited on a perfectly conducting substrate. The interface between the film and the substrate is assumed to be planar; the interface between the film and vacuum is a random grating (Fig. 20). The random surface in this case is the analogue of the deep random phase screen, while the perfect conductor is the analogue of the mirror, Jakeman's work.

The interest in studying the scattering of light from this structure is due to the fact that in the earliest numerical simulation studies of the scattering of p-polarized light from a random grating on a semi-infinite dielectric medium ($BaSO_4$) no enhanced backscattering was observed [7]. Subsequent calculations of the scattering of s-polarized light from the

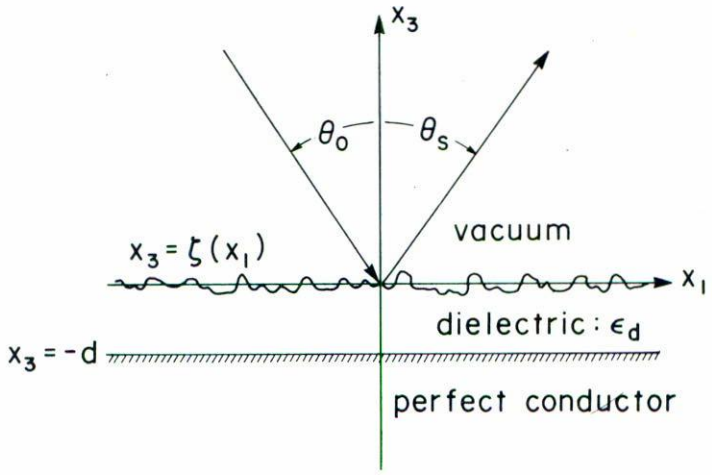

FIGURE 20. A nearly transparent dielectric film, with a random dielectric/vacuum interface, deposited on the planar surface of a perfect conductor (Ref. [15]).

same surfaces predicted enhanced backscattering [12]. In Ref. [11] it was shown that if the dielectric medium were made more reflective, by artificially doubling its index of refraction, then enhanced backscattering was observed in p-polarization as well. It was later found that a more modest increase of the index of refraction, viz. by a factor of 1.4–1.5, was sufficient to induce enhanced backscattering in p-polarization [12]. The question that the calculation described in the preceding paragraph would address, then, is whether the effective reflectivity of a dielectric medium with a random surface can be increased sufficiently, by depositing it in the form of a film on a highly reflecting substrate, to induced enhanced backscattering of p-polarized light from it.

We have carried out numerical simulations of the scattering of light of both p- and s-polarizations from the structure depicted in Fig. 20. The interface between the film and the vacuum was assumed to be a one-dimensional random surface defined by a surface profile function $\zeta(x_1)$ that is a Gaussianly distributed random variable with the properties $\langle\zeta(x_1)\rangle = 0$, $\langle\zeta(x_1)\zeta(x_1')\rangle = \delta^2 \exp(-(x_1 - x_1')^2/a^2)$. The details of how these calculations were carried out are presented in Ref. [15]. In Fig. 21 we present our results for the angular distribution of the incoherent component of p-polarized light scattered from a dielectric film of mean thickness $d = 4.8$ μm. Its roughness is characterized by the parameters $\delta = 1.2$ μm and $a = 2$ μm. The wavelength of the incident light is $\lambda = 0.6328$ μm, the index of refraction of the dielectric film at this wavelength if $n_d = 1.628 + i0.0003$. A total of $N_p = 1000$ profiles was used in obtaining this result. The angle of incidence is $\theta_0 = 20°$. A sharp peak is seen in $\langle\partial R_p/\partial\theta_s\rangle_{\text{incoh}}$ in the retroreflection direction $\theta_s = -20°$. For comparison, we present in Fig. 21b the result for $\langle_p/\partial_s\rangle_{\text{incoh}}$ obtained for exactly the same experimental conditions and roughness parameters except that the dielectric is now semi-infinite. No enhanced backscattering is seen in this case.

We believe that the enhanced backscattering we observe in these results can be explained in much the same way as the enhanced backscattering predicted by Jakeman [69] in the scattering of light from a deep random phase screen placed in front of a plane mirror

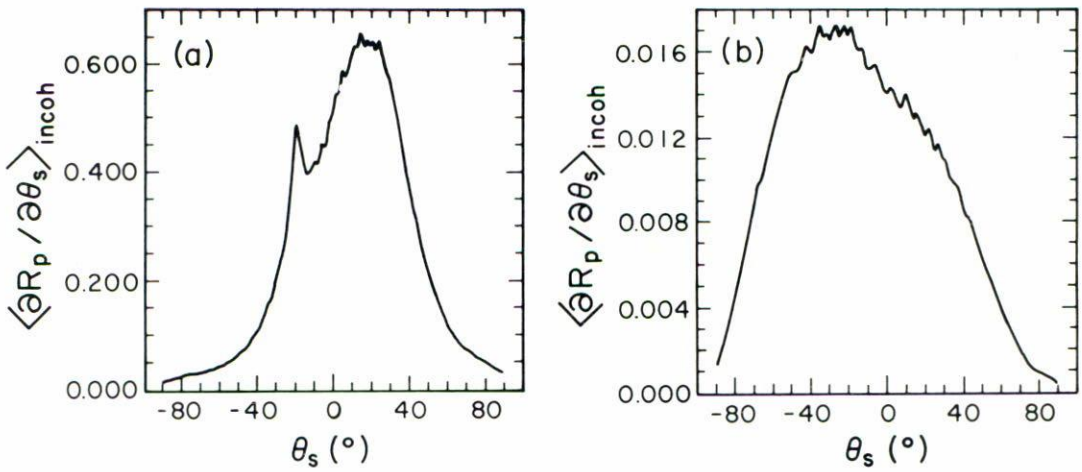

FIGURE 21. (a) The contribution to the mean differential reflection coefficient from the incoherent component of the scattered light when p-polarized light is incident on a random grating on the surface of $BaSO_4$ deposited on a perfectly conducting substrate. $\theta_0 = 20°$, $\lambda = 0.6328$ μm, $n_d = 1.628 + i0.0003$. $\delta = 1.2$ μm, $a = 2$ μm, $g = 6.4$ μm, $L = 25.6$ μm, $N = 300$, $N_p = 1000$. (b) Same as in (a) except that the random grating is on a semi-infinite $BaSO_4$ substrate (Ref. [15]).

can be explained. In the system studied by Jakeman, when the mirror is placed well beyond the focusing plane of the random phase screen the coherent addition of the contribution from a given light path that interacts with the random phase screen at two different points and its time reversed partner, Fig. 22a, leads to an enhancement of up to a factor of two in the intensity of light scattered into the backward direction. The angular width of this peak is determined by a transverse scattering length, which is the characteristic distance between the points on the random phase screen through which the light paths from the source pass and repass in being scattered into the retroreflection direction. When the mirror is placed closer to the random phase screen than the focusing plane of the latter, enhancement occurs because of a second passage through the same lenslike portion of the screen of light rays that have been focused on the mirror. A random "cat's eye" or corner cube effect then occurs, Fig. 22b, which gives rise to an incoherent backscattering enhancement of geometrical origin. This is a broad feature in comparison with the coherent enhancement, being comparable to the geometrical spread of rays scattered by the phase screen [71]. The enhancement produced by this single scattering mechanism is largest when the mirror is placed in the focusing plane of the random phase screen, and can be larger than the maximum factor of two enhancement produced by the coherent effect.

In the present context we need only replace "random phase screen" by "random surface" and "mirror" by "perfect conductor" to apply Jakeman's explanation to the results presented here.

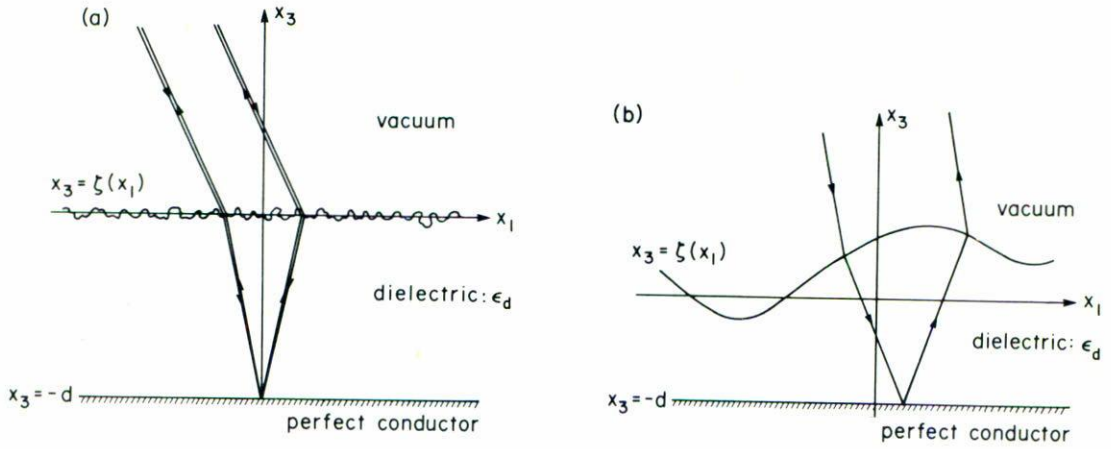

FIGURE 22. Mechanisms for the enhanced backscattering of light from a random grating on the surface of a dielectric film deposited on the planar surface of a perfectly conducting substrate: (a) coherent enhancement; (b) incoherent, geometrical enhancement (Ref. [15]).

We assume that the distance from the mean surface of the dielectric, $x_3 = 0$, to its focusing plane, $x_3 = \ell_f$, is given by $\ell_f = \rho n_d/(n_d - 1)$, which is the focal length of a thick cylindrical lens whose radius of curvature is ρ and whose index of refraction is n_d, which is illuminated by a line source that is infinitely distant from the lens. For the radius of curvature ρ we use the reciprocal of the rms curvature of the random grating surface, $\rho = \langle(\zeta''(x_1))^2\rangle^{-1/2} = (a^2/\delta)/(2\sqrt{3})$ for the Gaussian form for $W(|x_1|)$ used in this work. If we use the values of n_d, δ and a that entered the calculations of the results presented in Fig. 21, we find that $\ell_f = 2.4945$ μm, so that the perfect conductor is located at a distance from the random grating that is about 1.92 times the distance of the focusing plane from the random grating. It appears as if it is the coherent scattering process described by Jakeman (Fig. 22a) that is responsible for the enhanced backscattering observed in the results presented in Fig. 21.

In these calculations values of the mean film thickness d were used that were at least four times the value of the rms height of the surface roughness δ. This was because for such large values of the film thickness the probability of obtaining values of $|\zeta(x_1)|$ larger than d, which would produce "holes" in the film, is reduced to a negligible level. However, the use of films of such thicknesses made it impossible to place the perfect conductor much closer to the random surface than about $\frac{1}{2}\ell_f$. As a result, we could no demonstrate definitively the operation of Jakeman's second mechanism for enhanced backscattering from this structure. Results not presented here, however, fail to show an enhancement of more than a factor of two when the perfect conductor is placed in the focusing plane of the random surface.

The effect described in this section has been observed experimentally. In Fig. 23 we present experimental results for the mean differential reflection coefficient for the scattering of p-polarized light from a dielectric film on a gold substrate. The wavelength of the incident light is $\lambda = 0.6328$ μm, the index of refraction of the film is $n_d = 1.41$,

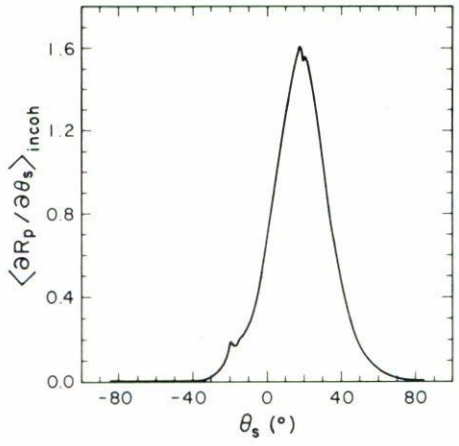

FIGURE 23. An experimental result for the contribution to the mean differential reflection coefficient from the incoherent component of the scattered light when p-polarized light is incident on a random grating on the surface of a dielectric film deposited on a planar gold substrate. $\theta_0 = 20°$, $\lambda = 0.6328$ μm, $n_d = 1.41$, $d = 8.5$ μm. $\delta = 1.08$ μm, $a = 3.06$ μm.

the mean thickness of the film is $d = 8.5$ mm The angle of incidence is $\theta_0 = 20°$. The roughness of the illuminated surface of the dielectric film is characterized by the parameters $\delta = 1.08$ μm and $a = 3.06$ μm. Although gold is not a perfect conductor under the conditions of the experiment, it is highly reflecting, and the consequence of this is that a peak in the retroreflection direction, $\theta_s = -20°$, is seen in the angular dependence of the intensity of the incoherent component of the scattered light. Despite the differences between the parameters defining the theoretical and experimental results, a comparison of the differential reflection coefficients presented in Figs. 21 and 23 shows them to be qualitatively similar.

2.3.2 Enhanced backscattering from a free-standing dielectric film

Once it has been realized that enhanced backscattering from a random dielectric surface can be induced or strengthened by depositing the dielectric in the form of a film on the surface of a reflecting medium, it is natural to inquire as to whether one can dispense with the reflecting substrate and use the (much weaker) reflection from the back face of a free-standing dielectric film in vacuum to achieve a similar effect. The answer turns out to be affirmative. We have calculated the contribution to the mean differential reflection coefficient from the incoherent component of the scattered light for light of p- and s-polarization incident on a $BaSO_4$ film of mean thickness 4.8 μm, whose illuminated surface is a random variable, with a Gaussian height correlation function characterized by the roughness parameters $\delta = 1.2$ μm and $a = 2$ μm. The wavelength of the incident light is 0.6328 μm, and the index of refraction of $BaSO_4$ at this wavelength is $n_c = 1.628 + i0.0003$. The results for an angle of incidence $\theta_0 = 20°$ are presented in Fig. 24. A total of $N_p = 3000$ surface profiles was used in obtaining these results. For both polarizations a well-defined peak is observed in $\langle R_{p,s}/\partial\theta_s \rangle_{\text{incoh}}$ at the scattering angle corresponding to

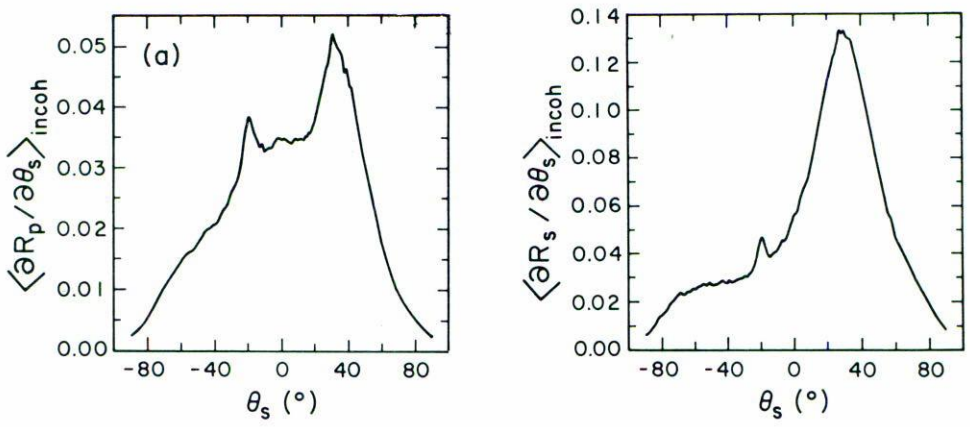

FIGURE 24. The contribution to the mean differential reflection coefficient from the incoherent component of the scattered light in the scattering of light of wavelength $\lambda = 0.6328$ μm from a random grating on a free-standing $BaSO_4$ film whose back surface is planar. $\theta_0 = 20°$, $n_d = 1.628 + i0.0003$. $\delta = 1.2$ μm, $a = 2$ μm, $d = 4.8$ μm. $g = 6.4$ μm, $L = 25.6$ μm, $N = 300$, $N_p = 3000$. (a) p-polarization; (b) s-polarization.

retroreflection, $\theta_s = -20°$. It should be noted that the overall scattered intensity in the case of p-polarized light is about twice what it is in the case of p-polarized light. Essentially the same result has been found earlier in the scattering of p- and s-polarized light from a one-dimensional random surface on a semi-infinite dielectric medium [7,12]. It should also be noted that the overall scattered intensity in the case of a free-standing dielectric film is lower by an order of magnitude than it is when the same film is deposited on a perfectly conducting substrate. This is due, of course, to the fact that only a small fraction of the light passing through the film and striking the back surface, is reflected back from it, in contrast with the total reflection that occurs in the case of a perfectly conducting substrate. Nevertheless, it is enough to induce enhanced backscattering in p-polarization where it is absent in the scattering from the surface of a semi-infinite dielectric medium. We believe that the mechanism responsible for this effect is the one depicted schematically in Fig. 22a in connection with the scattering of light from a rough dielectric film on a perfectly conducting substrate.

3. TWO-DIMENSIONAL RANDOM SURFACES

The random surfaces we have studied up to now in this paper have all been one-dimensional. In this section we turn to an investigation of the enhanced backscattering of light from two-dimensional random surfaces on metallic and nearly transparent dielectric substrates.

The scattering of light from two-dimensional random surfaces in richer in the effect to which it gives rise than is the scattering of light from one-dimensional surfaces. This

is due in part to the fact that cross-polarized scattering can occur from such surfaces in addition to the co-polarized scattering familiar in the scattering from one-dimensional random surfaces when the plane of incidence is normal to the generators of the latter surfaces. Cross-polarized scattering refers to the fact that even when the plane of scattering coincides with the plane of incidence, p-(s-)polarized light incident on a two-dimensional random surface produces scattered light that contains a component that is s-(p-)polarized. The theoretical and experimental study of cross-polarized scattering is of interest, because perturbation-theoretic calculations of the scattering of light from a two-dimensional random surface [3] show that one has to calculate the amplitude of the scattered field to second order in the surface profile function before in-plane, cross-polarized scattering is obtained. Consequently, it is not a single-scattering phenomenon but a multiple-scattering effect. As a result, one expects that enhanced backscattering calculated and observed in in-plane cross-polarized scattering should display the factor of two enhancement expected from the coherent interference of each multiply-reflected light path with its time-reversed partner, when the contribution from the single-scattering processes is subtracted, since the latter is not subject to coherent backscattering. This subtraction is not possible in co-polarized scattering, because the single-scattering contribution in this case is not known independently, but it occurs automatically in cross-polarized scattering, because, the latter contains no single-scattering contribution.

In this section we solve the problem of the scattering of light from two-dimensional random surfaces by a method that differs significantly from the one used in studying the scattering of light from one-dimensional random surfaces in the earlier sections of his article. We therefore conclude this introduction to the present section with a brief description of this method, and in Sects. 3.1 and 3.2 present the results obtained by its use for the scattering of light from two-dimensional random metallic and dielectric surfaces, respectively.

The system we study consists of vacuum in the region $x_3 > \zeta(\vec{x}_\parallel)$, and a metal or dielectric medium in the region $x_3 < \zeta(\vec{x}_\parallel)$, where $\vec{x}_\parallel = \hat{x}_1 x_1 + \hat{x}_2 x_2$ with $\hat{x}_1$ and $\hat{x}_2$ unit vectors along the x_1- and x_2-axes, respectively. We assume that the surface profile function $\zeta(\vec{x}_\parallel)$ is a stationary, stochastic, Gaussian process, defined by the properties

$$\langle \zeta(\vec{x}_\parallel) \rangle = 0, \tag{3.1}$$

$$\langle \zeta(\vec{x}_\parallel) \zeta(\vec{x}'_\parallel) \rangle = \delta^2 \exp(-|\vec{x}_\parallel - \vec{x}'_\parallel|^2/a^2), \tag{3.2}$$

where as before the angle brackets denote an average over the ensemble of realizations of the surface profile and $\delta = \langle \zeta^2(\vec{x}_\parallel) \rangle^{1/2}$ is the rms height of the surface.

A square segment of random surface of edge L in the x_1x_2-plane with the properties (3.1)-(3.2) is generated by an extension of the method described, *e.g.*, in Appendix A of Ref. [12]. It is then replicated periodically to cover the entire x_1x_2-plane. In this way a bigrating is created, albeit one with a very complicated period. The surface profile function is now a periodic function of x_1 and x_2 with a period L in each direction, and we expand it in a Fourier series,

$$\zeta(\vec{x}_\parallel) = \sum_{\vec{G}} \hat{\zeta}(\vec{G}) e^{i\vec{G}\cdot\vec{x}_\parallel}, \tag{3.3}$$

where $\vec{G} = (2\pi/L)(n_1, n_2)$ $(n_1, N_2 = 0, \pm 1, \pm 2, \ldots)$ is a vector of the two-dimensional lattice reciprocal to the square of lattice constant L.

The electric field in the vacuum above the random surface $(x_3 > \zeta(\vec{x}_\parallel)_{\max})$ is the sum of an incident field and of a scattered field,

$$\vec{E}(\vec{x}; t) = \vec{E}^{(i)}(\vec{x}; t) + \vec{E}^{(s)}(\vec{x}; t), \tag{3.4}$$

where

$$\vec{E}^{(i)}(\vec{x}; t) = \left\{ \frac{c}{\omega}[-\hat{K}_0 \alpha_0(K_0\omega) - \hat{x}_3 K_0] B_\parallel(\vec{K}_0\omega) + (\hat{x}_3 \times \hat{K}_0) B_\perp(\vec{K}_0\omega) \right\}$$

$$\times \exp[i(\vec{K}_0 - \hat{x}_3 \alpha_0(K_0\omega)) \cdot \vec{x} - i\omega t], \tag{3.5a}$$

$$\vec{E}^{(s)}(\vec{x}; t) = \sum_{\vec{K}} \left\{ \frac{c}{\omega}[-\hat{K}\alpha_0(K\omega) - \hat{x}_3 K] A_\parallel(\vec{K}\omega) + (\hat{x}_3 \times \hat{K}) A_\perp(\vec{K}\omega) \right\}$$

$$\times \exp[i(\vec{K} + \hat{x}_3 \alpha_0(K\omega)) \cdot \vec{x} - i\omega t]. \tag{3.5b}$$

In these expressions the subscripts $\parallel$ and $\perp$ denote the p-polarized (TM) and s-polarized (TE)-components of each of the fields, respectively. The two-dimensional wave vector $\vec{K}_0 = \hat{x}_1 k_1 + \hat{x}_2 k_2$ is the projection of the wave vector of the incident light on the plane $x_3 = 0$, the vector $\vec{K}$ is given by $\vec{K} = \vec{K}_0 + \vec{G}$, and the function $\alpha_0(K\omega)$ is defined by

$$\alpha_0(K\omega) = \left(\frac{\omega^2}{c^2} - K^2 \right)^{1/2} \qquad K^2 < \frac{\omega^2}{c^2} \tag{3.6a}$$

$$= i \left(K^2 - \frac{\omega^2}{c^2} \right)^{1/2} \qquad K^2 > \frac{\omega^2}{c^2}. \tag{3.6b}$$

If we write the relations between $A_\alpha(\vec{K}\omega)$ and $B_\beta(\vec{K}_0\omega)(\alpha, \beta = \parallel, \perp)$ in the form

$$A_\alpha(\vec{K}\omega) = \sum_\beta R_{\alpha\beta}(\vec{K}|\vec{K}_0) B_\beta(\vec{K}_0\omega), \tag{3.7}$$

then it can be shown that the mean differential reflection coefficient for the scattering of light of β-polarization, the projection of whose wave vector on the plane $x_3 = 0$ is $\vec{K}_0$, into light of α-polarization, the projection of whose wave vector on the plane $x_3 = 0$ is $\vec{K}$, is given by

$$\left\langle \frac{\partial R}{\partial \Omega_s} \right\rangle_{\substack{\alpha\beta \\ \text{incoh}}} = \left(\frac{L}{2\pi} \right)^2 \frac{\omega}{c} \frac{\alpha_0^2(K\omega)}{\alpha_0(K_0\omega)} [\langle |R_{\alpha\beta}(\vec{K}|\vec{K}_0)|^2 \rangle - |\langle R_{\alpha\beta}(\vec{K}|\vec{K}_0) \rangle|^2], \tag{3.8}$$

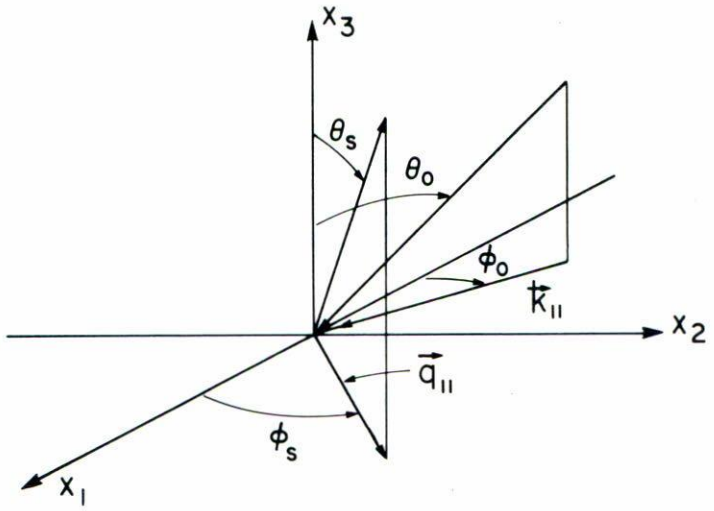

FIGURE 25. The scattering geometry for the scattering of light from a two-dimensional random surface.

where $\vec{K}_0 = (\omega/c)(\sin\theta_0\cos\phi_0, \sin\theta_0\sin\phi_0, 0)$ and $\vec{K} = (\omega/c)(\sin\theta_s\cos\phi_s, \sin\theta_s\sin\phi_s, 0)$, in terms of the angles of incidence (θ_0, ϕ_0) and scattering (θ_s, ϕ_s), respectively (Fig. 25). Only the contribution to the mean differential reflection coefficient from the incoherent component of the scattered light is present in the result given by Eq. (3.8).

A computationally much more tractable computational problem is obtained if we write $F_{\alpha\beta}(\vec{K}|\vec{K}_0)$ in the form

$$R_{\alpha\beta}(\vec{K}|\vec{K}_0) = R^{(0)}_{\alpha\beta}(\vec{K}|\vec{K}_0) - 2iG^{(0)}_{\alpha}(K\omega)T_{\alpha\beta}(\vec{K}|\vec{K}_0)G^{(0)}_{\beta}(K_0\omega)\alpha_0(K_0\omega), \tag{3.9}$$

where $\overleftrightarrow{R}^{(0)}$ is the 2×2 diagonal matrix of Fresnel coefficients for the scattering of p- and s-polarized light from a planar surface,

$$\overleftrightarrow{R}^{(0)}(\vec{K}|\vec{K}_0) = \delta_{\vec{K},\vec{K}_0}\begin{pmatrix} \dfrac{\epsilon(\omega)\alpha_0(K\omega) - \alpha(K\omega)}{\epsilon(\omega)\alpha_0(K\omega) - (K\omega)} & 0 \\ 0 & \dfrac{\alpha_0(K\omega) - \alpha(K\omega)}{\alpha_0(K\omega) + \alpha(K\omega)} \end{pmatrix}, \tag{3.10}$$

with $\alpha(K\omega) = (\epsilon(\omega)(\omega^2/c^2) - K^2)^{1/2}$ $(\mathrm{Re}\,\alpha(K\omega) > 0, \mathrm{Im}\,\alpha(K\omega) > 0)$, while $G^{(0)}_p(K\omega) = i\epsilon(\omega)/[\epsilon(\omega)\alpha_0(k\omega) + \alpha(K\omega)]$, $G^{(0)}_s = i/[\alpha_0(K\omega) + \alpha(K\omega)]$ are the Green's functions for surface electromagnetic waves on a planar vacuum-dielectric interface. The scattering matrix $T_{\alpha\beta}(\vec{K}|\vec{K})$ is postulated to satisfy the equation

$$T_{\alpha\beta}(\vec{K}|\vec{K}) = V_{\alpha\beta}(\vec{K}|\vec{K}') + \sum_{\vec{K}'\gamma} V_{\alpha\gamma}(\vec{K}|\vec{K}')G^{(0)}_{\gamma}(K'\omega)T_{\gamma\beta}(\vec{K}'|\vec{K}_0), \tag{3.11}$$

where to first order in the surface profile function the effective scattering potential matrix $\overleftrightarrow{V}(\vec{K}|\vec{K}')$ is given by [43]

$$\overleftrightarrow{V}(\vec{K}|\vec{K}') = \hat{\zeta}(\vec{K}-\vec{K}')\frac{\epsilon(\omega)-1}{\epsilon^2(\omega)} \times \begin{pmatrix} \epsilon(\omega)KK' - \alpha(K\omega)(\hat{K}\cdot\hat{K}')\alpha(K'\omega) & -\frac{\omega}{c}\alpha(K\omega)(\hat{K}\times\hat{K}')_3 \\ -\frac{\omega}{c}(\hat{K}\times\hat{K}')_3\alpha(K'\omega) & \epsilon(\omega)\frac{\omega^2}{c^2}(\hat{K}\cdot\hat{K}') \end{pmatrix} \tag{3.12}$$

The approximation represented by Eq. (3.12) is the small roughness approximation, and its use restricts the validity of the results obtained to two-dimensional random surfaces with small rms slopes. The contribution to the mean differential reflection coefficient from the incoherent component of the scattered light, Eq. (3.8), can now be rewritten as

$$\left\langle \frac{\partial R}{\partial \Omega_s} \right\rangle_{\substack{\alpha\beta \\ \text{incoh}}} = \left(\frac{L}{2\pi}\right)^2 4\frac{\omega}{c}\alpha_0(K\omega)\{\alpha_0(K\omega)|G_\alpha^{(0)}(K\omega)|^2 \times [\langle|T_{\alpha\beta}(\vec{K}|\vec{K}_0|^2\rangle - |\langle T_{\alpha\beta}(\vec{K}|\vec{K}_0)\rangle|^2]\,|G_\beta^{(0)}(K_0\omega)|^2\,\alpha_0(K_0\omega)\}. \tag{3.13}$$

We now note that $G_p^{(0)}(K\omega)$ has a pole at the wave vectors $k_\parallel$ for which the equation

$$\epsilon\alpha_0(K\omega) + \alpha(K\omega) = 0$$

is satisfied. This is just the dispersion relation for p-polarized surface electromagnetic waves at the planar interface between vacuum and a dielectric medium whose dielectric constant is ϵ. We exploit the resulting resonant behavior of $G_p^{(0)}(K\omega)$ for K in the vicinity of these wave vectors to make a pole approximation for $G_p^{(0)}(K\omega)$:

$$G_p^{(0)}(K\omega) \cong C_1\left[\frac{1}{K - K_{sp} - i\Delta_\epsilon} - \frac{1}{K + K_{sp} + i\Delta_\epsilon}\right], \tag{3.14}$$

where Δ_ϵ is the rate of damping of the surface electromagnetic wave due to ohmic losses, *i.e.*, to the imaginary part of the dielectric constant. The explicit expressions for C_1, K_{sp}, and Δ_ϵ depend on whether the dielectric medium is a metal or a nearly transparent medium, and will be given in Secs. 3.2 and 3.3, respectively.

We also note that $G_s^{(0)}(K\omega)$ has no such pole, because the dispersion relation for s-polarized surface electromagnetic waves at the planar interface between vacuum and a dielectric medium $\alpha_0(K\omega) + \alpha(K\omega) = 0$, has not solution [72]. In what follows, therefore, we will neglect the nonresonant Green's function $G_s^{(0)}(K\omega)$, and will keep only the resonant function $G_p^{(0)}(K\omega)$.

Equation (3.11) is now solved by using the pole approximation and solving for the T-matrix of the resonant channels by inverting the matrix equations

$$T_{pp}(\vec{K}_r|\vec{K}_0) = V_{pp}(\vec{K}_r|\vec{K}_0) + \sum_{\vec{K}'_r} V_{pp}(\vec{K}_r|\vec{K}'_r)G_p^{(0)}(K'_r\omega)T_{pp}(\vec{K}_r|\vec{K}_0), \tag{3.15a}$$

$$T_{ps}(\vec{K}_r|\vec{K}_0) = V_{ps}(\vec{K}_r|\vec{K}_0) + \sum_{\vec{K}'_r} V_{pp}(\vec{K}_r|\vec{K}'_r)G_p^{(0)}(K'_r\omega)T_{ps}(\vec{K}'_r|\vec{K}_0). \tag{3.15b}$$

The sum over $\vec{K}'_r$ is restricted to the resonant channels, which we consider to be any $\vec{K}$ within $2\Delta_\epsilon$ of K_{sp}. The other T-matrix elements are then obtained from Eq. (3.11) in the pole approximation,

$$T_{\alpha\beta}(\vec{K}|\vec{K}_0) = V_{\alpha\beta}(\vec{K}|\vec{K}_0) + \sum_{\vec{K}_r} V_{\alpha p}(\vec{K}|\vec{K}_r)G_p^{(0)}(K_r\omega)T_{p\beta}(\vec{K}_r|\vec{K}_0). \tag{3.16}$$

Note that $G_s^{(0)}(K\omega)$ does not enter any of these calculations because it is never resonant.

Equations (3.15)-(3.16) were solved for $T_{\alpha\beta}(\vec{K}|\vec{K}_0)$ and the results used in calculating $\langle \partial R/\partial\Omega_s\rangle_{\substack{\alpha\beta \\ \text{incoh}}}$ from Eq. (3.13), for a large number of different surface profiles for each of several values of L. The use of different values of L was to obtain a more nearly continuous distribution of values of the (in fact discrete) scattering angles θ_s and ϕ_s than can be obtained with a single value of L. However, for a given $\vec{K}_0$ the value of L was always chosen in such a way that one of the $\vec{K}$'s coincided with the backscattering channel, $-\vec{K}_0$. This was necessary because the angular width of the peak in the mean differential reflection coefficient in the retroreflection direction is comparable with or smaller than the angular resolution of the present calculations, which is limited by the values of L that we were able to use. Consequently, to observe enhanced backscattering it was necessary to ensure that the retroreflection direction was always one of the allowed scattering angles.

3.1 Metallic surfaces [17]

In studying the scattering of light from a two-dimensional, random metallic surface, we assume that the region $x_3 < \zeta(\vec{x}_\parallel)$ is filled by a metal that is characterized by an isotropic, complex, frequency-dependent, dielectric constant $\epsilon(\omega) = \epsilon_1(\omega) + i\epsilon_2(\omega)$. We assume further that we are working in a frequency range in which $\epsilon_1(\omega)$ is negative, *i.e.* in the frequency range in which surface polaritons can exist, and that the inequalities $|\epsilon_1(\omega)| \gg 1 \gg \epsilon_2(\omega) > 0$ are satisfied.

To obtain the pole approximation to $G_p^{(0)}(K\omega)$ in this case we start from the identity

$$G_p^{(0)}(K\omega) = \frac{i\epsilon(\omega)}{\epsilon(\omega)\alpha_0(K\omega) + \alpha(K\omega)} = i\epsilon(\omega)\frac{\epsilon(\omega)\alpha_0(K\omega) - \alpha(K\omega)}{\epsilon^2(\omega)\alpha_0^2(K\omega) - \alpha^2(K\omega)}$$

$$= \frac{i\epsilon(\omega)}{1-\epsilon^2(\omega)}\frac{\epsilon(\omega)\alpha_0(K\omega) - \alpha(K\omega)}{2K_0(\omega)}\left[\frac{1}{K - K_0(\omega)} - \frac{1}{K + K_0(\omega)}\right], \tag{3.17}$$

where

$$K_0(\omega) = \frac{\omega}{c}\left(\frac{\epsilon(\omega)}{\epsilon(\omega)+1}\right)^{1/2}$$

$$\cong \frac{\omega}{c}\left(\frac{|\epsilon_1(\omega)|}{|\epsilon_1(\omega)|-1}\right)^{1/2}\left[1+\frac{i}{2}\frac{\epsilon_2(\omega)}{|\epsilon_1(\omega)|(|\epsilon_1(\omega)|-1)}\right], \tag{3.18}$$

to lowest nonzero order in $\epsilon_2(\omega)$. Our notation emphasizes the fact that we are concerned with the frequency range in which $\epsilon_1(\omega) < 0$. The values of $\alpha_0(K\omega)$ and $\alpha(K\omega)$ evaluated at $K = \pm K_0(\omega)$ are

$$\alpha_0(\omega) = i\frac{\omega}{c}\frac{1}{(|\epsilon_1(\omega)|-1)^{1/2}}\left[1+\frac{i}{2}\frac{\epsilon_2(\omega)}{|\epsilon_1(\omega)|-1}\right], \tag{3.19a}$$

$$\alpha(\omega) = i\frac{\omega}{c}\frac{|\epsilon_1(\omega)|}{(|\epsilon_1(\omega)|-1)^{1/2}}\left[1-\frac{i}{2}\frac{|\epsilon_1(\omega)|-2}{|\epsilon_1(\omega)|(|\epsilon_1(\omega)|-1)}\right], \tag{3.19b}$$

where the signs of the square roots of complex numbers have been chosen in such a way that $\alpha_0(\omega)$ reduce to the correct expressions when $\epsilon_2(\omega) \to 0$. When these results are used in evaluating the residue at the poles $K = \pm K_0(\omega)$, we find that $G_p^{(0)}(K\omega)$ takes the form given by Eq. (3.14) with

$$C_1 = \frac{|\epsilon_1(\omega)|^{3/2}}{|\epsilon_1(\omega)|^2-1}, \tag{3.20a}$$

$$K_{sp} = \frac{\omega}{c}\left(\frac{|\epsilon_1(\omega)}{|\epsilon_1(\omega)|-1}\right)^{1/2}, \tag{3.20b}$$

$$\Delta_\epsilon = \frac{i}{2}\frac{\epsilon_2(\omega)}{|\epsilon_1(\omega)|(|\epsilon_1(\omega)|-1)}K_{sp}. \tag{3.20c}$$

In Fig. 26 we show typical results for the contribution to the mean differential reflection coefficient from the incoherent component of the scattered light for in-plane cross-polarized scattering of s-polarized (Fig. 26a) and p-polarized (Fig. 26b) light incident normally on a two-dimensional random silver surface [17]. The assumption of normal incidence in these calculations ensures that the retroreflection direction is always one of the allowed scattering directions. The wavelength of the incident light was $\lambda = 4579$ Å, and the dielectric constant of silver at his wavelength is $\epsilon(\omega) = -7.5 + i0.24$. The roughness of the surface was characterized by the values $\delta = 50$ Åand $a = 1200$ Å. The results presented were obtained from 500 realizations for each of 45 values of L distributed between 9140 nm and 9700 nm. The value of Δ_ϵ^{-1} in this case is 27563 nm. They show a backscattering enhancement that is as pronounced for a two-dimensional random surface as it is for a one-dimensional random profile. In fact, the height of the enhanced backscattering peak

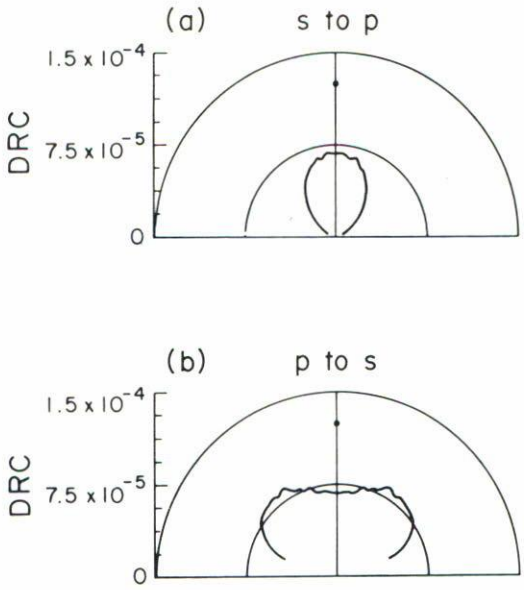

FIGURE 26. Polar plots of the contribution to the mean differential reflection coefficient from the incoherent of the scattered light for the in-plane, cross-polarized scattering of light incident normally on a two-dimensional, random silver surface. $\lambda = 0.4579$ μm, $\epsilon(\omega) = -7.5 + i0.24$. $\delta = 50$ Å, $a = 1200$ Å. The intensity in the backscattering channel is shown by a heavy dot (Ref. [17]).

is very close to the expected factor of two greater than the height of the background at its position. These results are in general agreement with those of the diagrammatic theory of McGurn and Maradudin [3].

3.2 Dielectric surfaces [24]

It has been shown by numerical simulations carried out in Refs. [11] and [12] that enhanced backscattering can be observed in the scattering of p-polarized light from a semi-infinite dielectric medium if the real part of the index of refraction of the medium is positive and sufficiently large. Some insight into why this should be so was provided in recent work by Antsygina *et al.* [73]. They pointed out that a planar interface between vacuum and a nearly transparent dielectric medium can support a surface polariton provided the real part of the dielectric constant is positive and sufficiently large, and the imaginary part is not too small. The binding of this wave to the surface is due to the imaginary part of the dielectric constant, and the curve of ω vs Rek in this case lies to the left of the light line, *i.e.* in the radiative region of the ω, k-plane. Antsygina *et al.* [73] used this result as the basis for a pole approximation to the Green's functions that arise in the perturbation-theoretic approach to enhanced backscattering [1-3], and by means of a calculation similar to that of Ref. 1, for scattering from a one-dimensional random metallic surface showed that a weakly rough dielectric surface can also display this effect.

To see how this effect comes about, we now assume that the region $x_3 < \zeta(\vec{x}_\parallel)$ is filled by a dielectric medium characterized by an isotropic, frequency-independent, complex, dielectric constant $\epsilon = \epsilon_1 + i\epsilon_2$, and assume that ϵ_1 and ϵ_2 satisfy the inequalities $\epsilon_1 \gg 1 \gg \epsilon_2 > 0$. To obtain the function C_1, K_{sp} and Δ_ϵ that enter the pole approximation (3.14) for $G_p^{(0)}(K\omega)$ we first need to find the zeros of the equation $\epsilon\alpha_0(K\omega) + \alpha(K\omega) = 0$, *i.e.*, the poles of $G_p^{(0)}(K\omega)$. To analyze this equation and its solutions it is convenient to make the placement $K^2 = (\omega^2/c^2)(1 - z)$, after which this equation becomes

$$S(z) \equiv \epsilon z^{1/2} + (z - (1 - \epsilon))^{1/2} = 0. \tag{3.21}$$

The problem of obtaining K from a solution z of Eq. (3.21) is simplified by the fact that we seek an electromagnetic wave that propagates in the x_1-direction and is attenuated in the direction of propagation. Thus, if we assume ω real and K complex, $K = K_R + iK_I$, then both K_R and K_I must be positive. These requirements tell us which sign of the square root of $1 - z$ gives the physically acceptable solution. The square roots in the expression for $S(z)$ given by Eq. (3.21) give rise to two branch points in the complex z-plane at $z = 0$ and $z = 1 - \epsilon$. We take as branch cuts the line $(\infty, 0)$ for $z = 0$, and $(-\infty - i\epsilon_2, 1 - \epsilon_1 - i\epsilon_2)$ for $(z - (1 - \epsilon))^{1/2}$. The Riemann surface on which $S(z)$ is single-valued consists of four sheets, each of which is defined by a combination of sheets of $z^{1/2}$ and $(z-(1-\epsilon))^{1/2}$. These can be denoted by $S_1 = (+,+)$, $S_2 = (+,-)$, $S_{-1} = (-,-)$, $S_{-2} = (-,+)$, according to $(\text{sgn Re}\, z^{1/2}, \text{sgn Re}(z - (1 - \epsilon))^{1/2})$.

There are no physically acceptable solutions of Eq. (3.21) on the sheets S_1 and S_{-1}, because the real part of $S(z)$ cannot vanish in this case. The only physically acceptable solution is found on the sheet $S_{-2} = (-,+)$. In the case of interest here, viz. $\epsilon_1 \gg 1 \gg \epsilon_2 > 0$, it is given by

$$z \cong \frac{1}{\epsilon_1 + 1} - i\frac{\epsilon_2}{(\epsilon_1 + 1)^2}, \tag{3.22}$$

from which it follows that

$$K = \frac{\omega}{c}\left(\frac{\epsilon_1}{\epsilon_1 + 1}\right)^{1/2}\left[1 + i\frac{\epsilon_2}{2\epsilon_1(\epsilon_1 + 1)}\right]. \tag{3.23}$$

The corresponding expressions for $\alpha_0(\omega)$ and $\alpha(\omega)$ are

$$\alpha_0(\omega) = \frac{\omega}{c}\left[-\frac{1}{(\epsilon_1 + 1)^{1/2}} + i\frac{\epsilon_2}{2(\epsilon_1 + 1)^{3/2}}\right] \tag{3.24a}$$

$$\alpha(\omega) = \frac{\omega}{c}\frac{\epsilon_1}{(\epsilon_1 + 1)^{1/2}}\left[1 + i\frac{\epsilon_2(\epsilon_1 + 2)}{2\epsilon_1(\epsilon_1 + 1)}\right]. \tag{3.24b}$$

It is the fact that $\text{Im}\,\alpha_0(\omega)$ and $\text{Im}\,\alpha(\omega)$ are positive, due to the positivity of both ϵ_1 and ϵ_2, that demonstrates the binding of the wave in each medium to the surface $x_3 = 0$. The solution found on the sheet $S_2(+,-)$ has both $\text{Im}\,\alpha_0(\omega)$ and $\text{Im}\,\alpha(\omega)$ negative, and

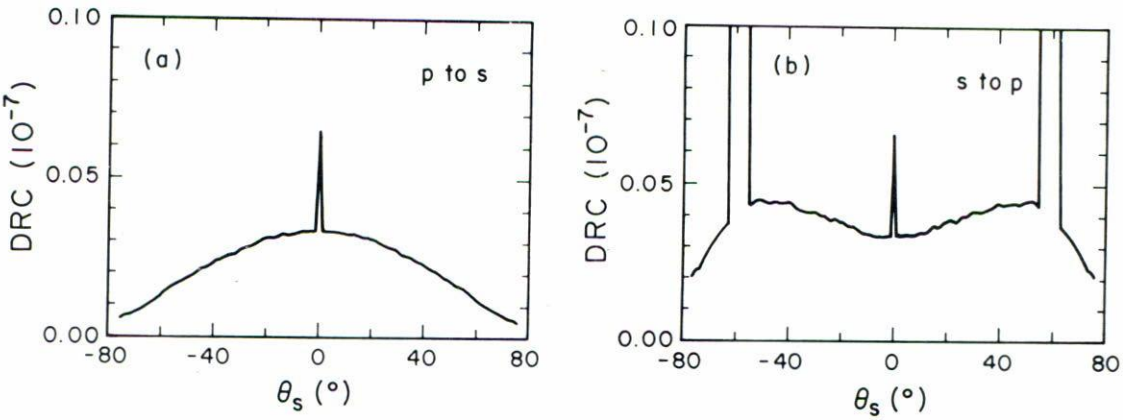

FIGURE 27. The contribution to the mean differential reflection coefficient from the incoherent component of the scattered light for the in-plane, cross-polarized scattering of light incident normally on a two-dimensional, random dielectric surface. $\lambda = 0.4579$ Å, $\epsilon(\omega) = 2.65 + i0.1$, $\delta = 10$ Å, $a = 1000$ Å (Ref. [24]).

is therefore unacceptable. Thus, unlike surface polaritons, which are bound to the surface $x_3 = 0$ by the negativity of ϵ_1, the wave described by Eqs. (3.23)-(3.24) is bound because of the ohmic losses in the dielectric medium, *i.e.* because ϵ_2 is nonzero and positive. The surface electromagnetic waves that exist at a planar vacuum-dielectric interface when the conditions $\epsilon_1 \gg 1 \gg \epsilon_2 > 0$ are satisfied are sometimes referred to as *Brewster modes* [74].

With the preceding results in hand and Eq. (3.17) it is now straightforward to show that the quantities C_1, K_{sp}, and Δ_ϵ in the pole approximation for $G_p^{(0)}(K\omega)$ are given by

$$C_1 = \frac{i\epsilon_1^{3/2}}{\epsilon_1^2 - 1}, \tag{3.25a}$$

$$K_{sp} = \frac{\omega}{c}\left(\frac{\epsilon_1}{\epsilon_1 + 1}\right)^{1/2}, \tag{3.25b}$$

$$\Delta_\epsilon = \frac{\epsilon_2}{2\epsilon_1(\epsilon_1 + 1)} K_{sp}. \tag{3.25c}$$

In Fig. 27 we present the contribution to the mean differential reflection coefficient from the incoherent component of the light scattered from a two-dimensional, random, dielectric surface. The light is incident normally on the surface, and only the results for in-plane cross-polarized scattering are shown. The wavelength of the incident light is $\lambda = 4579$ Å, and the dielectric constant of the scattering medium is $\epsilon = 2.65 + i0.1$. The roughness of

the surface was characterized by the values $\delta = 10$ Å and $a = 1000$ Å. The plots were obtained by averaging the results of calculations for 18 values of L ranging from 13625 nm to 13975 nm. (The value of Δ_ϵ^{-1} in this case was 16546 nm). 500 realizations of the surface were used for each value of L. As in the case of scattering from a metal surface discussed in Sec. 3.1, the assumption of normal incidence in these calculations ensured that the retroreflection direction was always one of the allowed scattering directions. Well-defined peaks in the retroreflection direction are observed in the mean differential reflection coefficient for the scattering of p-polarized light into s-polarized light, Fig. 27a, and for the scattering of s-polarized light into p-polarized light, Fig. 27b. The angular widths of these peaks, however, are due to the finite angular resolution of these calculations, resulting from our use of values of L that are smaller than Δ_ϵ^{-1}, and are not the true widths of these peaks, which are smaller. The height of the enhanced backscattering peak in each case is very close to a factor of 2 larger than the height of the background at its position.

4. Discussion and conclusions

Several conclusions can be drawn from the results presented in this article.

The existence of enhanced backscattering from moderately rough, reflecting, random surfaces that scatter light multiply appears not to depend in an essential way on the nature of the surface profile function. Provided that these surfaces scatter light multiply, enhanced backscattering occurs for a variety of forms of the surface height correlation function; it occurs for band-limited fractal surfaces, which are characterized by two transverse length scales, as well as for surfaces characterized by a single transverse length scale; it occurs for surfaces whose surface profile function is not a Gaussianly distributed random variable; and it occurs for surfaces that are characterized by a surface profile function that is not a stationary stochastic process. These results strongly suggest that the dominant property of a moderately rough, reflecting surface that is responsible for enhanced backscattering is its ability to scatter the incident light multiply. Other properties of such surfaces may affect the details of the dependence of the mean differential reflection coefficient on the scattering angle, but not the existence of enhanced backscattering itself.

The result that the angular width of the enhanced backscattering peak is inversely proportional to the mean distance between consecutive peaks and valleys on a one-dimensional random surface, which was established for a single-scale surface defined by a Gaussian surface height correlation function and was implied by the results for a band-limited fractal surface, is significant for the following reason. As van Albada *et al.* [40] have emphasized, enhanced backscattering has been known for a long time, and a number of possible explanations for it, not involving interference, have been proposed and discussed [40]. For example, enhanced backscattering may result from shadowing (only in the exact backscattering direction does one not see scatterers that are located in the shadow of other scatterers); it may be due to lens action (dew drops may focus sunlight onto a plant leaf and refract much of the scattered light into the backward direction); or it may be due to retroreflection (a corner cube effect). Thus, the observation of enhanced backscattering by itself does not establish its origin in weak localization. To make that connection one must prove that it results from interference. The inverse dependence of

the angular width of the enhanced backscattering peak on the mean free path of the light along the surface, which we have related to the mean distance between consecutive peaks and valleys on the surface, seems to be a good criterion for doing so.

In the case of a weakly rough, one-dimensional surface that supports surface electromagnetic waves the results of Sec. 2.2.1 show that when a magnetic field is applied parallel to the generators of the surface and the frequency of the incident light is in the range in which both forward ($k > 0$) and backward ($k < 0$) propagating surface polaritons exist, the position of the enhanced backscattering peak is shifted in the direction of larger (in magnitude) scattering angles and the peak is washed out as the magnetic field strength is increased. These results are in qualitative agreement with the predictions of the perturbation-theoretic calculations of enhanced backscattering in a magnetic field presented in Ref. [16]. In addition, they show that when the frequency of the incident light is in the range in which only forward propagating ($k > 0$) surface polaritons exist no enhanced backscattering is observed. The present calculations do not assume a special role for the surface polaritons supported by the semiconductor/vacuum interface in the formation of the enhanced backscattering peak, as the perturbation-theoretic calculations of Ref. [16] did, through their use of a pole approximation for the Green's functions entering the scattering calculations. The roughness of the surfaces studied in the present work is weak enough that multiple scattering of light from them is improbable. Thus, the agreement between the results of the present numerical simulations and the perturbation-theoretic results of Ref. [16] is seen as support for the suggestion that the dominant mechanism responsible for enhanced backscattering from weakly rough surfaces is the coherent interference of each multiply-scattered surface polariton path with its time-reversed partner. The shift in the position of the enhanced backscattering peak and the destruction of enhanced backscattering with increasing magnetic field strength are then due to the nonreciprocity of these surface polaritons caused by the application of the external magnetic field and the consequent loss of coherency between surface polariton paths and their time-reversed partners.

It is also worth noting that the displacement of the position of the enhanced backscattering peak from the retroreflection direction, when the frequency of the incident light is in the range where both forward and backward propagating, nonreciprocal surface polaritons exist at the frequency, may help to make enhanced backscattering easier to study experimentally, by removing the necessity of having the detector adjacent to the light source.

The results obtained in Sec. 2.2.2 for the enhanced backscattering of light from a periodic metallic grating perturbed by random roughness, and presented in Figs. 18 and 19, show that enhanced backscattering occurs when the frequency of the incident light falls in a range in which surface polaritons exist, but is strongly suppressed when the frequency of the incident light falls in a range in which surface polaritons cannot exist. These results are additional strong evidence for the essential role played by these surface electromagnetic waves in the formation of enhanced backscattering from weakly rough random surfaces.

Taken together, the results of Secs. 2.2.1 and 2.2.2 leave no doubt that the origin of the enhanced backscattering predicted [1,2,12] and observed [27] in the scattering of light

from very smooth, random metal surfaces is the roughness-induced multiple scattering of the surface polaritons excited by the incident light through the surface roughness.

A moderately rough random surface on a transparent dielectric medium which does not display enhanced backscattering of p-polarized light when the medium is semi-infinite, does so when the same surface bounds a thin film of the dielectric material deposited on the planar surface of a highly reflecting material. The observed enhanced backscattering from this structure is believed to be due to the coherent interference of a light path that passes through the random surface twice, due to its reflection from the substrate, with its time-reversed partner. In effect, the presence of the reflecting substrate ensures the double-scattering of the incident light from the random surface that is primarily responsible for enhanced backscattering.

This double passage of a light path through the random surface still occurs if the highly reflecting substrate is removed, leaving a free-standing dielectric film whose illuminated face is a random surface while its back face is planar. In this case it is the much weaker reflection of the light from the planar backface of the film that accomplishes this. Yet this weaker reflection is enough to induce enhanced backscattering from a random surface that does not display the effect when it bounds a semi-infinite dielectric medium.

In our analytic-cum-numerical studies of enhanced backscattering of light from small rms slope, two-dimensional, random metallic and dielectric surfaces we have shown that the mechanism involved in each case is the scattering of the surface electromagnetic waves on the corresponding surface by the roughness of that surface. Because cross-polarized scattering in the plane of incidence can only occur by multiple scattering, the peaks observed in Figs. 26 and 27 are multiple-scattering phenomena. Because there is no contribution to the mean differential reflection coefficient from single-scattering processes in this case, we expect that the height of the enhanced backscattering peak should be twice the height of the background at its position, for the reason given in the Introduction to this article. This is indeed what is observed in the results presented in Figs. 26 and 27.

Experimental results for the in-plane cross-polarized scattering of light from random, two-dimensional random surface of a dielectric, MgO have been obtained by Kim *et al.* [29]. They observed enhanced backscattering and were able to show that it is a multiple-scattering effect. The ratio of the height of the enhanced backscattering peak relative to the height of the background at its position is close to the factor of two observed in the results depicted in Fig. 27. However, the surfaces they studied were very rough. It is therefore not clear whether surface electromagnetic waves exist on these surfaces and, if so, how much they contribute to the enhanced backscattering of light.

ACKNOWLEDGEMENTS

This article is based on an invited talk given by A.A.M. at the annual meeting of the Mexican Physical Society and the Academy of Optics of Mexico, held in Ensenada, Baja California, Mexico, October 22-26, 1990. It describes work done in collaboration with the other authors of this article. A.A.M. is grateful to the organizers of the meeting for the invitation to present this talk, and to the Editorial Board of the Revista Mexicana de Fisica for the invitation to publish this written version of the talk in the Journal. He

is also grateful to Professor V. Tognetti and Professor S. Califano for the hospitality of the Department of Physics of the University of Florence and of the European Laboratory for Nonlinear Spectroscopy, respectively, where this article was written. This research was supported in part by ARO Grants DAAL-88-K-0067 and DAAL-03-89-C-0036, and by NATO Grant 890528. It was also supported by the University of California, Irving, through an allocation of computer time.

REFERENCES

1. A.R. McGurn, A.A. Maradudin, and V. Celli, *Phys. Rev.* **B31** (1985) 4866.
2. V. Celli, A.A. Maradudin, A.M. Marvin and A.R. McGurn, *J. Opt. Soc. Am.* **A2** (1985) 2225.
3. A.R. McGurn and A.A. Maradudin, *J. Opt. Soc. Am.* **B4** (1987) 910.
4. E. Bahar and M.A. Fitzwater, *Optics Commun.* **63** (1987) 355.
5. M. Nieto-Vesperinas and J.M. Soto-Crespo, *Optics Lett.* **12** (1987) 979.
6. P. Tran and V. Celli, *J. Opt. Soc. Am.* **A5** (1988) 1635.
7. A.A. Maradudin, E.R. Méndez and T. Michel, *Optics Lett.* **14** (1989) 151.
8. T. Michel, A.A. Maradudin and E.R. Méndez, *J. Opt. Soc. Am.* **B6** (1989) 2438.
9. M. Nieto-Vesperinas and J.M. Soto-Crespo, *Phys. Rev.* **B39** (1989) 8193.
10. E. Bahar and M.A. Fitzwater, *J. Opt. Soc. Am.* **A6** (1989) 33.
11. A.A. Maradudin, E.R. Méndez and T. Michel, in *Scattering in Volumes and Surfaces*, eds. M. Nieto-Vesperinas and J.C. Dainty, North-Holland, Amsterdam (1990) p. 157.
12. A.A. Maradudin, T. Michel, A.R. McGurn and E.R. Méndez, *Ann. Phys. (N.Y.)* **203** (1990) 255.
13. Jin Ya-Qiu and M. Lax, *Phys. Rev.* **B42** (1990) 9819.
14. C. Macaskill, *J. Opt. Soc. Am.* **A8** (1991) 88.
15. Jun Q. Lu, A.A. Maradudin and T. Michel, *J. Opt. Soc. Am.* **B8** (1991) 311.
16. A.R. McGurn, A.A. Maradudin and R.F. Wallis, *Waves in Random Media* **1** (1991) 43.
17. V. Celli, P. Tran, A.A. Maradudin, Jun Lu, T. Michel and Zu-Han Gu, in *Laser Optics of Condensed Matter*, Vol. 2, eds. E. Garmire, A.A. Maradudin, and K.K. Rebane, Plenum, New York (1991) p. 315.
18. A. Ishimaru, J.S. Chen, P. Phu and K. Yoshitomi, *Waves in Random Media* **1** (1991) S91.
19. A.A. Maradudin, Jun Q. Lu, T. Michel, Zu-Han Gu, J.C. Dainty, A.J. Sant, E.R. Méndez and M. Nieto-Vesperinas, *Waves in Random Media* **1** (1991) S129.
20. D. Maystre, M. Saillard and J. Ingres, *Waves in Random Media* **1** (1991) S143.
21. M. Nieto-Vesperinas, J.A. Sánchez-Gil and A.A. Maradudin, *Waves in Random Media* **1** (1991) S157.
22. E. I. Thorsos and D.R. Jackson, *Waves in Random Media* **1** (1991) S165.
23. Jun Q. Lu, A.A. Maradudin and R.F. Wallis, *Waves in Random Media* **1** (1991) 309.
24. P. Tran, A.A. Maradudin and V. Celli, *J. Opt. Soc. Am.* **B 8** (1991) 1526.
25. E.R. Méndez and K.A. O'Donnell, *Optics Commun.* **61** (1987) 91.
26. K.A. O'Donnell and E.R. Méndez, *J. Opt. Soc. Am.* **A4** (1987) 1194.
27. Zu-Han Gu, R.S. Dummer, A.A. Maradudin and A.R. McGurn, *Appl. Optics* **28** (1989) 537.
28. J.C. Dainty, M.J. Kim and A.J. Sant, in *Scattering in Volumes and Surfaces*, eds. M. Nieto-Vesperinas and J.C. Dainty, North-Holland, Amsterdam (1990) p. 143.
29. M.J. Kim, J.C. Dainty, A.T. Friberg and A.J. Sant, *J. Opt. Soc. Am.* **A7** (1990) 569.
30. J.C. Dainty, N.C. Bruce and A.J. Sant, *Waves in Random Media* **1** (1991) S29.
31. G. Bergmann, *Phys. Rev.* **B28** (1983) 2914.
32. D.E. Khmel'nitskii, *Physica* **126B** (1984) 235.

33. E. Abrahams, P.W. Anderson, D.C. Licciardello and T.V. Ramakrishnan, *Phys. Rev. Lett.* **42** (1979) 673.
34. P.W. Anderson, *Phys. Rev.* **109** (1958) 1493.
35. A good discussion of the localization of classical waves can be found in *Scattering and Localization of Classical Waves in Random Media*, ed. P. Sheng, World Scientific, Singapore (1990).
36. Y. Kuga and A. Ishimaru, *J. Opt. Soc. Am.* **A1** (1984) 831.
37. M.P. van Albada and A. Lagendijk, *Phys. Rev. Lett.* **55** (1985) 2692.
38. P.E. Wolf and G. Maret, *Phys. Rev. Lett.* **55** (1985) 2696.
39. L. Tsang and A. Ishimaru, *J. Opt. Soc. Am.* **A1** (1984) 836; **A2** (1985) 1331; **2** (1985) 2187.
40. M.P. van Albada, M.B. van der Mark, and A. Lagendijk, in *Scattering and localization of classical waves in random media*, ed. P. Sheng, World Scientific, Singapore (1990) p. 97.
41. N.E. Glass, A.A. Maradudin and V. Celli, *Phys. Rev.* **B27** (1983) 5150.
42. N.E. Glass, A.A. Maradudin and V. Celli, *J. Opt. Soc. Am.* **73** (1983) 1240.
43. G.C. Brown, V. Celli, M. Haller, and A. Marvin, *Surf. Sci.* **136** (1984) 381.
44. F. Toigo, A. Marvin, V. Celli and N.R. Hill, *Phys. Rev.* **B15** (1977) 5618.
45. M.E. Knotts and K.A. O'Donnell, *Optics Lett.* **15** (1990) 1485.
46. E.R. Méndez, M.A. Ponce, V. Ruíz-Cortés and Zu-Han Gu, *Applied Optics* **30** (1991) 4103.
47. A.J. Sant, J.C. Dainty and M.J. Kim, *Optics Lett.* **14** (1989) 1183.
48. M. Nieto-Vesperinas, J.A. Sánchez-Gil, A.J. Sant and C. Dainty, *Optics Lett.* **1t** (1990) 1261.
49. N. García and E. Stoll, *J. Opt. Soc. Am.* **A2** (1985) 2240.
50. See, for example, J.D. Jackson, *Classical Electrodynamics*, Wiley, New York (1962) pp. 14-15.
51. R.F. Harrington, *Field Computation by Moment Methods*, Macmillan, New York (1968).
52. A.A. Maradudin and T. Michel, *J. Stat. Phys.* **58** (1990) 485.
53. A.A. Maradudin and T. Michel, SPIE Proceedings 1558-26 (July, 1991).
54. J.M. Soto-Crespo and M. Nieto-Vesperinas, *J. Opt. Soc. Am.* **A6** (1989) 367.
55. M.V. Berry, *J. Phys.* **A12** (1979) 781.
56. M.G. Kivelson and S.A. Moszkowski, *J. Appl. Phys.* **36** (1963) 3609.
57. P. Beckmann, *IEEE Trans. Ant. Propag.* **AP-21** (1973) 169.
58. M.V. Berry, *J. Phys.* **A10** (1977) 2061.
59. G.S. Brown, *Radio, Sci.* **17** (1982) 1274.
60. E. Jakeman and B.J. Hoenders, *Opt. Acta* **29** (1982) 1587.
61. M.J. Kim, E.R. Méndez and K.A. O'Donnell, *J. Mod. Opt.* **34** (1987) 1107.
62. S.C. Wu, M.S. Chen and A.K. Fung, *IEEE Trans. Geosci. Remote Sensing* **26** (1988) 790.
63. S.C. Wu, M.S. Chen and A.K. Fung, *IEEE Trans. Geosci. Remote Sensing* **26** (1988) 885.
64. P.F. Gray, *Optica Acta* **25** (1972) 765.
65. R.F. Wallis, in *Electromagnetic Surface Modes*, ed. A.D. Boardman, Wiley, New York (1982) p. 575.
66. C.A. Condat, T.R. Kirkpatrick and S.M. Cohen, *Phys. Rev.* **B35** (1987) 4653.
67. J.S. Blakemore, *J. Appl. Phys.* **53** (1982) R123.
68. B. Laks, D.L. Mills and A.A. Maradudin, *Phys. Rev.* **B23** (1981) 4965.
69. E. Jakeman, *J. Opt. Soc. Am.* **A5** (1988) 1638.
70. P.R. Tapster, A.R. Weeks and E. Jakeman, *J. Opt. Soc. Am.* **A6** (1989) 517.
71. E. Jakeman, in *Scattering in Volumes and Surfaces*, eds. M. Nieto-Vesperinas and J.C. Dainty, North-Holland, Amsterdam (1990) p. 111.
72. See, for example, A.A. Maradudin, in *Surface Polaritons*, eds. V.M. Agranovich and D.L. Mills, North-Holland, Amsterdam (1982) p. 405.
73. T.A. Antsygina, V.D. Freylikher, S.A. Gredskul, L.A. Pastur and V.A. Slyusarev, *J. Electr. Waves Appl.* **5** (1991) 873.
74. P. Halevi, *Surf. Sci.* **76** (1978) 64.